geosciences

MDPI

Article

Paleo-Drainage Network, Morphotectonics, and Fluvial Terraces: Clues from the Verde Stream in the Middle Sangro River (Central Italy)

Enrico Miccadei [1,2,*], Cristiano Carabella [1], Giorgio Paglia [1] and Tommaso Piacentini [1,2]

[1] Department of Engineering and Geology, Università degli Studi "G. d'Annunzio" Chieti-Pescara, Viale Pindaro 42, 65127 Pescara, Italy; cristianocarabella12@gmail.com (C.C.); giorgiopaglia3@gmail.com (G.P.); tommaso.piacentini@unich.it (T.P.)

[2] Istituto Nazionale di Geofisica e Vulcanologia, Sezione Roma 1, Via di Vigna Murata 605, 00143 Rome, Italy

* Correspondence: enrico.miccadei@unich.it

Received: 18 July 2018; Accepted: 31 August 2018; Published: 8 September 2018

Abstract: This work analyzes the role of paleo-drainage network, morphotectonics, and surface processes in landscape evolution in a sector of the transition zone between the chain and the piedmont area of Central Apennines. Particularly, it focuses on the Verde Stream, a tributary of the middle Sangro River valley, which flows in the southeastern Abruzzo area at the boundary with the Molise region. The Verde Stream was investigated through a drainage basin scale geomorphological analysis incorporating the morphometry of the orography and hydrography, structural geomorphological field mapping, and the investigation of morphological field evidence of tectonics with their statistical azimuthal distributions. The local data obtained were compared with the analysis of the middle Sangro River valley and the tectonic features of the Abruzzo–Molise area. This approach led us to also provide relevant clues about the definition of the role of karst features and paleo-landscapes in the general setting of the study area and to identify the impact of active tectonics, confirmed by recent and active seismicity. In conclusion, the paper contributes to defining the main stages of the geomorphological evolution of this area, driven by uplift and local tectonics and due to a combination of fluvial, karst, and landslide processes.

Keywords: landscape evolution; drainage network; morphotectonics; fluvial terraces; karst morphogenesis; waterfalls; Central Italy

1. Introduction

The transition zone between the chain and the piedmont area of the Central Apennines is a key sector in the comprehension of the long-term landscape evolution of this chain [1–3]. Moreover, taking into account the ongoing formation of the Apennines orogeny, this sector is placed between the well-known extensional tectonics domain of the western inner part of the chain [4] and the compressional tectonics domain, affecting the eastern sectors along the Adriatic area with the interaction of the Adria microplate [5,6]. Additionally, it is experiencing a recent historical and active moderate-to-strong seismicity [6–8]. For this reason, this area experienced a strong uplift and it is largely characterized by deep dissection along transversal valleys [9–12] that cross the front of the chain along the main rivers (i.e., Tronto, Pescara, Sangro, Trigno, Biferno [2,12–16]) and it is usually mostly affected by denudational landforms and poorly characterized by continental deposits. Nevertheless, this transition zone can provide useful contributions in the comprehension of the landscape evolution, if investigated through an integrated morphotectonic analysis as documented in several studies along the Apennines and in other mountain ranges [17–22].

The middle Sangro River valley is located in the southeastern Abruzzo area at the boundary with the Molise region (Figure 1). This area is placed in the transition zone between the Central Apennines chain and its Adriatic piedmont. Moreover, it crosses, within the chain area, the boundary between the carbonate domain of the Abruzzo Apennines and the clayey–marly allochthonous domain of the Molise Apennines. It has been the subject of a scientific debate in terms of geological setting [23–25], complex allochthonous setting, tectonic features (thrusting vs. strike-slip), role of extensional tectonics [26–30], deep structures [6,31–33], lacking of geomorphological terraces [2,3,34], while the geomorphological investigations were mostly focused on the piedmont area [2,3,14–16,35,36] and in the inner mountain chain [34,37–40].

This work provides a contribution to the definition of the landscape features of this transition zone, resulting from morphotectonics and surface erosional–depositional (morphoscultural) processes, by means of surface investigations (i.e., field geomorphological investigations, terrain morphometry). It focuses on the analysis of the Verde Stream valley and of the middle Sangro River, characterized by general and local geomorphic indicators of tectonics and by different types of anomalies (e.g., drainage network anomalies, irregularities in long profiles, hanging landscapes, karst features, and a lack of fluvial terraces). The Verde Stream catchment area was analyzed following a methodology already applied in several studies of the main Adriatic rivers (e.g., [2,3,11,35,37,41,42]), which let to outline Quaternary tectonic features, even in areas where non-conservative lithologies do not allow for a good conservation of fault exposures and tectonic landforms, resulting in poor constraining of geometry and timing of the structures. The local results were compared with the analysis of the middle Sangro River valley through the comparison of paleo-landscapes, karst landforms, and fluvial terrace distribution along the Sangro's long profile. Karst landforms widely characterize the area surrounding the Verde Stream–Sangro River junction and, therefore, their contribution in the landscape evolution was evaluated. These features, largely underestimated in the studies on Quaternary landscape evolution, seem to increase their significance in the understanding the geomorphological evolution of the chain–piedmont transition zone [2,3,12,43].

Finally, the aim of this work is to give a contribute to the study of the impact of active tectonics and geomorphological processes (slope gravity and karst processes) on fluvial landscapes and river valley development in uplifting areas, characterized by Quaternary morphogenesis on erodible lithologies. The surface results may also provide a contribution to the comprehension of deep tectonic structures poorly evident but documented by recent and active seismicity [6–8].

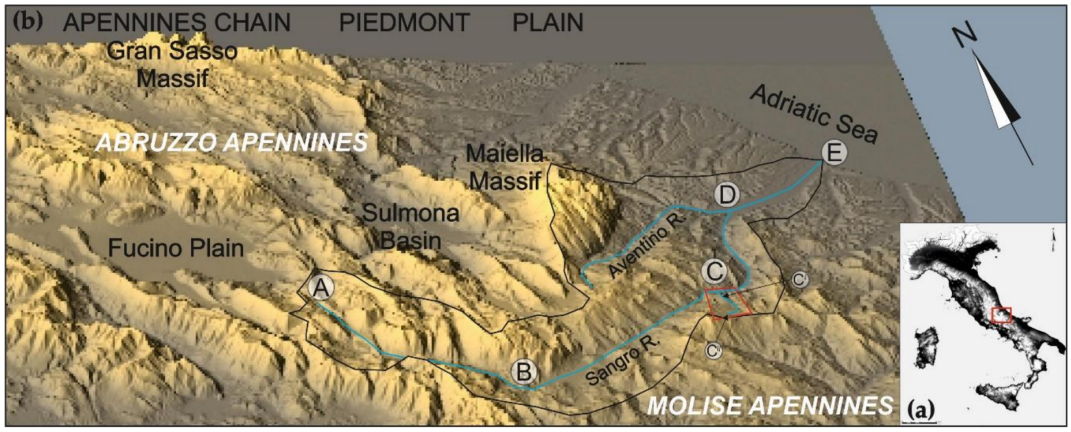

Figure 1. (**a**) Location map of the study area in Central Italy. (**b**) 3D view (from 90 m DEM, SRTM) of the Abruzzo–Molise region. Letters A, B, C, D, E outline key point of the Sangro River (i.e., main river bend and knick points); Letters C′ and C″ outline key point of the Verde Stream. In blue: the drainage network; in black: the drainage basin of the Sangro River; the red box frames the drainage basin object of this study (modified from [2]).

2. Study Area

2.1. Regional Geological and Geomorphological Setting

The Verde Stream is a tributary of the middle Sangro River valley, located at the boundary between the Abruzzo and the Molise Apennines (Central Italy) and at the transition zone between the chain and the piedmont area (Figure 1). The Central Apennines chain alternates ridges (up to 2900 m a.s.l. high: i.e., Gran Sasso massif, 2912 m a.s.l.; Maiella massif, 2793 m a.s.l.), longitudinal and transversal valleys (such as the Sangro River valley) and wide intermontane basins (i.e., Fucino Plain, Sulmona Basin) (Figure 1). It shows an asymmetric profile with the highest peaks towards NE from the main drainage divide [9,11,12]. The chain abruptly drops down to the piedmont area (ranging from ~600 m a.s.l. to the coast line), which features a gentle cuesta and mesa landscape incised by SW–NE cataclinal valleys [1,43]. The geological setting is the result of the Neogene–Quaternary evolution of an orogenic system (chain–foredeep–foreland) migrating eastward [44]. The geomorphological evolution began with the emersion of the orogen, forming an initial landscape, at least from the Miocene in the chain area and from the late Early Pleistocene in the piedmont area. The landscape is the result of the combination of tectonic processes (i.e., Miocene–Pliocene thrusting and Quaternary extensional tectonics), rock uplift and surface processes (e.g., slope, fluvial, karst, and glacial processes) [11,43].

The chain is made up of a thrust belt that involved Mesozoic–Cenozoic lithological sequences pertaining to different structural and paleo-geographical domains (carbonate platforms and related margins, slope, and pelagic basin) featuring different tectonic orientations. The carbonate platform domain (i.e., Abruzzo Apennines) is characterized by NW–SE to NNW–SSE-oriented thrusts (turning to N–S in the Sangro area, e.g., Maiella) developed from the Late Miocene to the Early Pliocene. The pelagic basin domain (i.e., Molise Apennines) features a chaotic assemblage on clayey–marly–limestone units developed along NW–SE-oriented Late Miocene–Pliocene compressional structures (e.g., Casoli–Bomba structure [32,33]). These structures caused the complex superimposition of carbonate tectonic units imbricate one over the other and over turbiditic foredeep sequences (Abruzzo Apennines) and the emplacement of allochthonous thrust sheets (Molise Apennines) [33,45,46]. The thrust sheets were affected and deformed by strike-slip tectonics along mostly NW–SE to NNW–SSE-oriented faults, poorly constrained in age and largely masked by later extensional tectonic events [28]. Since the Early Pleistocene (and more intensively during the Middle Pleistocene), the orogen was affected by extensional tectonics and regional uplifting, which led to the formation of the intermontane basins in the chain and the emersion of the Adriatic piedmont [1,11,12,47]. The piedmont area is characterized by the outer thrust sheets involving pelitic–arenaceous Neogene turbiditic foredeep sequences, which are largely covered and unconformably overlain by a Pleistocene clay–sand–conglomerate marine regressive sequence. This domain, emerged in the late Early Pleistocene, is affected by regional uplifting and presents a homocline setting and a cuesta-mesa-plateau relief carved by the main consequent river valleys arranged in SW–NE orientation roughly transversal to the Apennines chain and filled by flights of fluvial terraces (Figures 2 and 3). The combination of morphotectonics and surface processes results in the reorganization of drainage systems, the dismembering of the paleo-landscapes generated during the initial shaping stage, the development of several valleys with flights of fluvial terraces and the formation of the present-day landscape [9,11,12,43,48–50].

The present-day tectonic setting is dominated by extensional tectonics still active in the axial part of the chain, which is characterized by intense seismicity and strong historical earthquakes (up to M 7.0; e.g., Majella Massif 1706; Mts. Matese 1805; Fucino 1915; L'Aquila 2009). The Adriatic piedmont is characterized by moderate uplifting and moderate seismicity, while the Adriatic Sea is affected by subsidence and by moderate compression and strike-slip related seismicity [5,51]. The main tectonic orientation of the structures controlling the recent seismicity are again NW–SE (extensional faults in the Abruzzo Apennines [52]) and mostly E–W (strike-slip features in the Molise Apennines and piedmont area [28]) as also documented by the recent seismicity (i.e., August 2018 Molise earthquake [53]).

In this framework, the Sangro River valley, at the transition between NNW–SSE to N–S calcareous structural domain and NW–SE clayey–marly–calcareous domain, and the Verde tributary basin, at the transition between chain and piedmont area, deserve a detailed investigation for the comprehension of the geomorphological landscape evolution.

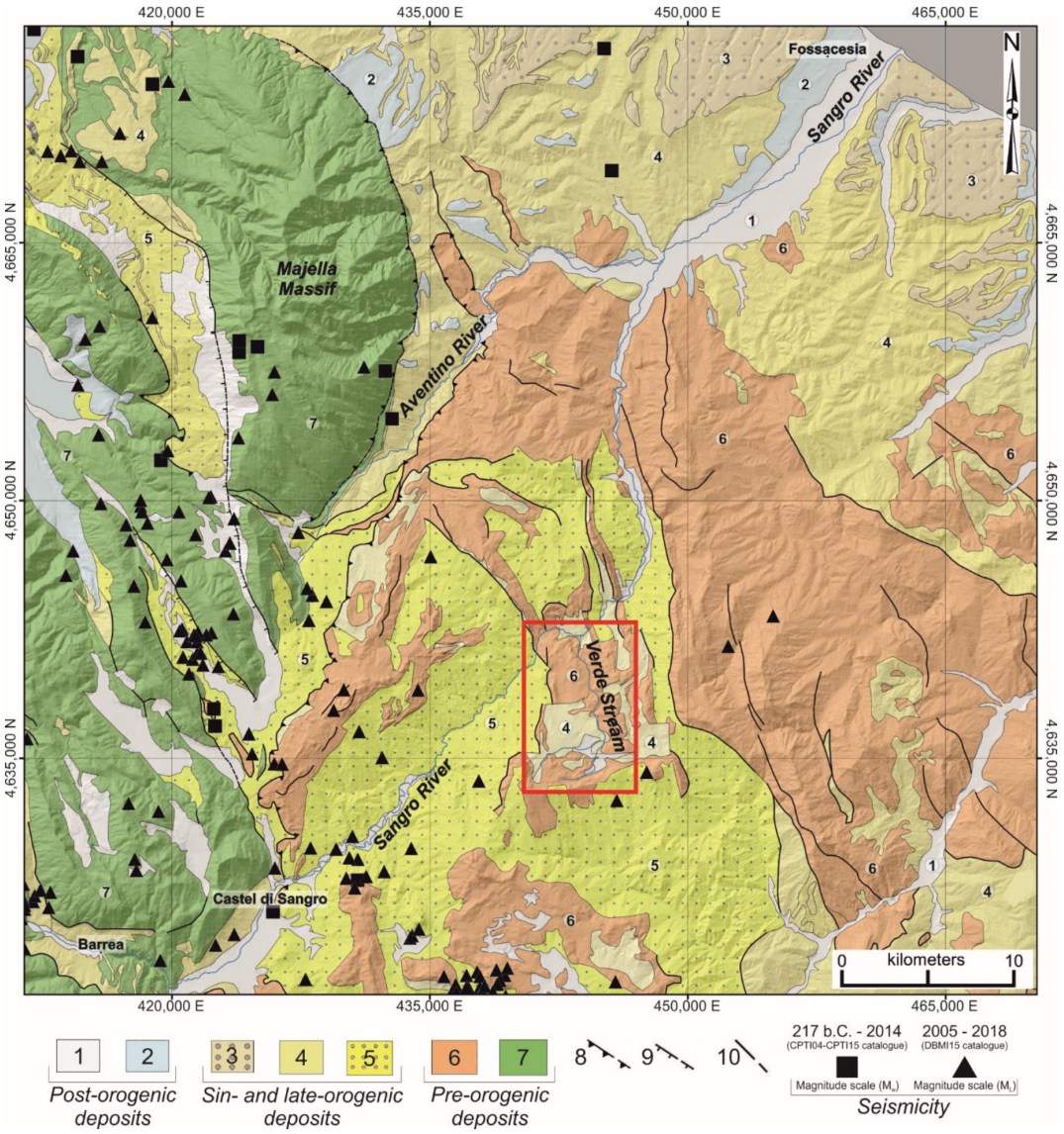

Figure 2. Geological scheme of southeastern Abruzzo (modified from [2]). Legend: post-orogenic Quaternary continental deposits, (1) fluvial deposits (Holocene), (2) terraced fluvial and alluvial fan deposits (Middle-Late Pleistocene); sin- and late-orogenic terrigenous deposits, (3) marine to continental transitional sequences (Early Pleistocene), (4) hemipelagic sequences with conglomerate levels (Late Pliocene–Early Pleistocene), (5) turbiditic foredeep sequences (Late Miocene–Early Pliocene); pre-orogenic carbonate, marly and clayey deposits, (6) Molise pelagic sequences (Oligocene–Miocene), (7) carbonate platform, slope and pelagic basin sequences (Jurassic–Miocene); (8) major thrust (dashed if buried); (9) major normal fault (dashed if buried); (10) major fault with strike-slip or reverse component (dashed if buried); seismicity, CPTI04 [54]-CPTI15 [7] catalogue (black square); DBMI15 [55] catalogue (black triangle). In blue: the drainage network; the red box frames the drainage basin object of this study.

The Sangro River is, at present, 107 km long and features variable orientations: from N–S in the upper reach, to WNW–ESE to SW–NE, to S–N, and, finally, to SW–NE in the lower reach. The present

drainage basin area is about 1560 km^2, of which ca. 70% lies within the chain area and the remaining 30% within the piedmont. The Sangro River's long profile (Figure 4a) can be divided into different reaches based on abrupt bends and/or long gradient variations. The first part shows a regular long-profile with a gradient value of 10–15 m/km. The intermediate reach shows a sharp knick zone marked convex shape with a gradient value of up to 45 m/km that roughly correspond to the transition zone between chain and piedmont domains. The lower reach incises, with a concave long profile, piedmont and coastal hilly area and presents a gradient value of 5–10 m/km [2]. The Sangro River crosses the Abruzzo–Molise Apennines. The upper and northern part of the basin is dominated by imbricated NNW–SSE to N–S thrust sheets developed from the Late Miocene to the Early Pliocene and formed by thick carbonate platform sequences, while the middle and southeastern part features NW–SE allochthonous thrust sheets on clayey–marly–calcareous pelagic basin sequences, both overlain by Neogene turbiditic foredeep sequences [1,24,45,56]. Finally, the lower part of the basin is on the Pleistocene marine regressive sequence.

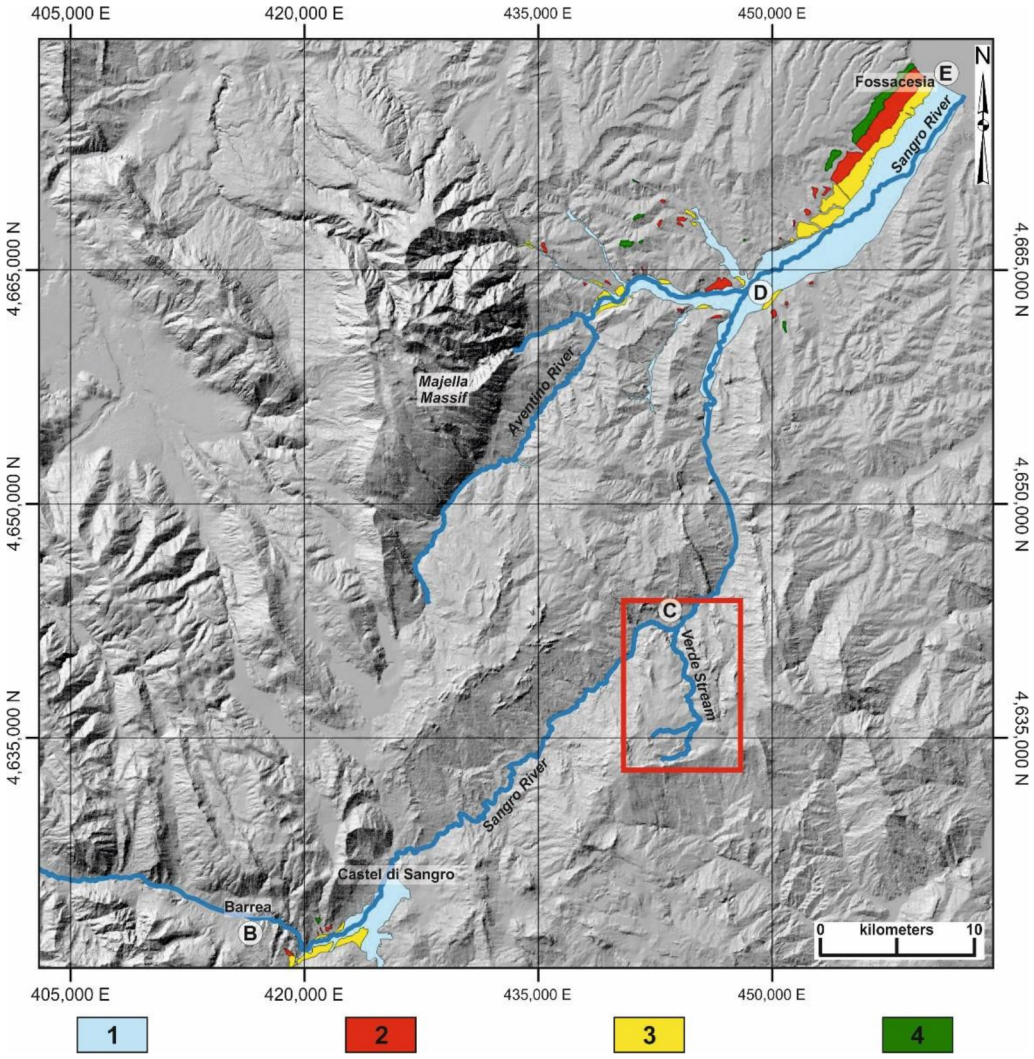

Figure 3. Fluvial terraces schema of the middle-lower Sangro River valley. In blue, the drainage network; the red box frames the drainage basin object of this work. Letters refer to Figure 1 (modified from [2,12,34]). Legend: (1) fourth order terrace—alluvial plane (Holocene); (2) third order terrace (Late Pleistocene); (3) second order terrace (late Middle Pleistocene); (4) first order terrace (Middle Pleistocene).

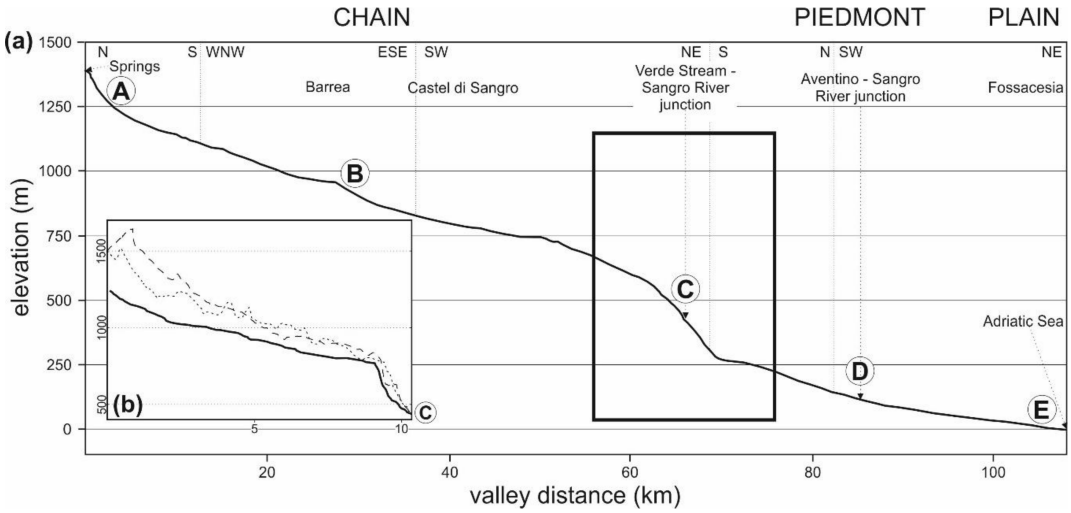

Figure 4. (**a**) Plot of the Sangro River's long profile and location of the study area (box) (modified from [2]); (**b**) Plot of the Verde Stream's long profile; stream profile is shown in black line; dotted line is the right side ridge-line profile; dashed line is left side ridge-profile. Location in Figure 1 (letters A, B, C, D, E).

The Quaternary continental deposits are widespread in the region, mainly consisting of fluvial, slope, and landslide deposits. The fluvial deposits, arranged in a sequence of four main fluvial terraces (Figures 2 and 3), are well preserved in the intermontane basins (i.e., Castel di Sangro basin) of the chain and in the piedmont area, while they are poorly preserved in the transition zone between the chain and the piedmont. These terraces are mostly of climatic origin and have been connected to the main cold climate stages of the Middle–Late Pleistocene (as all along the Apennines piedmont [2,14,36,48,57–59]) and are referred to the Middle Pleistocene (first order), Late Middle Pleistocene (second order), Late Pleistocene (third order) and Late Pleistocene–Holocene (fourth order, Figure 3) [2,48,60]. The Verde Stream is a tributary which flows into the middle Sangro River that features its highest steepness and a marked knick zone in the transition zone between the chain and the piedmont area.

2.2. Geological Setting of the Verde Stream Catchment Area

The Verde Stream valley is a hilly mountain area with a wavy and irregular morphology that progressively increases in terms of steepness moving towards the Sangro River junction. The main stream is as short as 11 km, flows first towards SW–NE and then around N–S and covers an elevation range of about 600 m (from ~1200 m a.s.l. to 420 m a.s.l.) with an average gradient of about 50 m/km. Its long profile (Figure 4b), similar to that of the Sangro River, is characterized by a gentle concave upper and mid reach (from 30 to 80 m/km) with slight undulations and a sharp knick zone passing to a very high gradient (~250 m/km) in the lower reach. This sector is marked by the presence of the Verde Waterfalls, the highest (~200 m) natural waterfall in the Italian peninsula. The bedrock geology (Figure 5) consists of Oligocene–Miocene marly, marly–calcareous, marly–arenaceous, and clayey successions (Argille varicolori formation [61–64]) and by an alternation of marly–calcareous, calcarenite and calcirudite rocks (Tufillo formation and Gamberale–Pizzoferrato formation [25,64]) pertaining to the Molise pelagic sequences. The carbonatic sequences are overlain by Upper Miocene–Early Pliocene pelitic and pelitic–arenaceous deposits (lower part of the Flysch di Agnone formation [61,62,64]). Bedrock sequences are overlain by Late Pleistocene and Holocene continental deposits (Figure 5) that are widespread and mainly represented by landslide (chaotic gravelly deposits), fluvial (gravel–alluvial deposits), lacustrine (clays and clay–silt deposits), and karst deposits (red soils) [1,26,27,61,62,64,65]. Finally, the study area shows a homoclinal tectonic setting with a gentle eastward dipping attitude bounded by complex inverse tectonic contacts. The structural axis is mainly N–S with ENE–WSW strike-slip faults and minor NNW–SSE normal faults cutting the major tectonic structures [26,27,31,65].

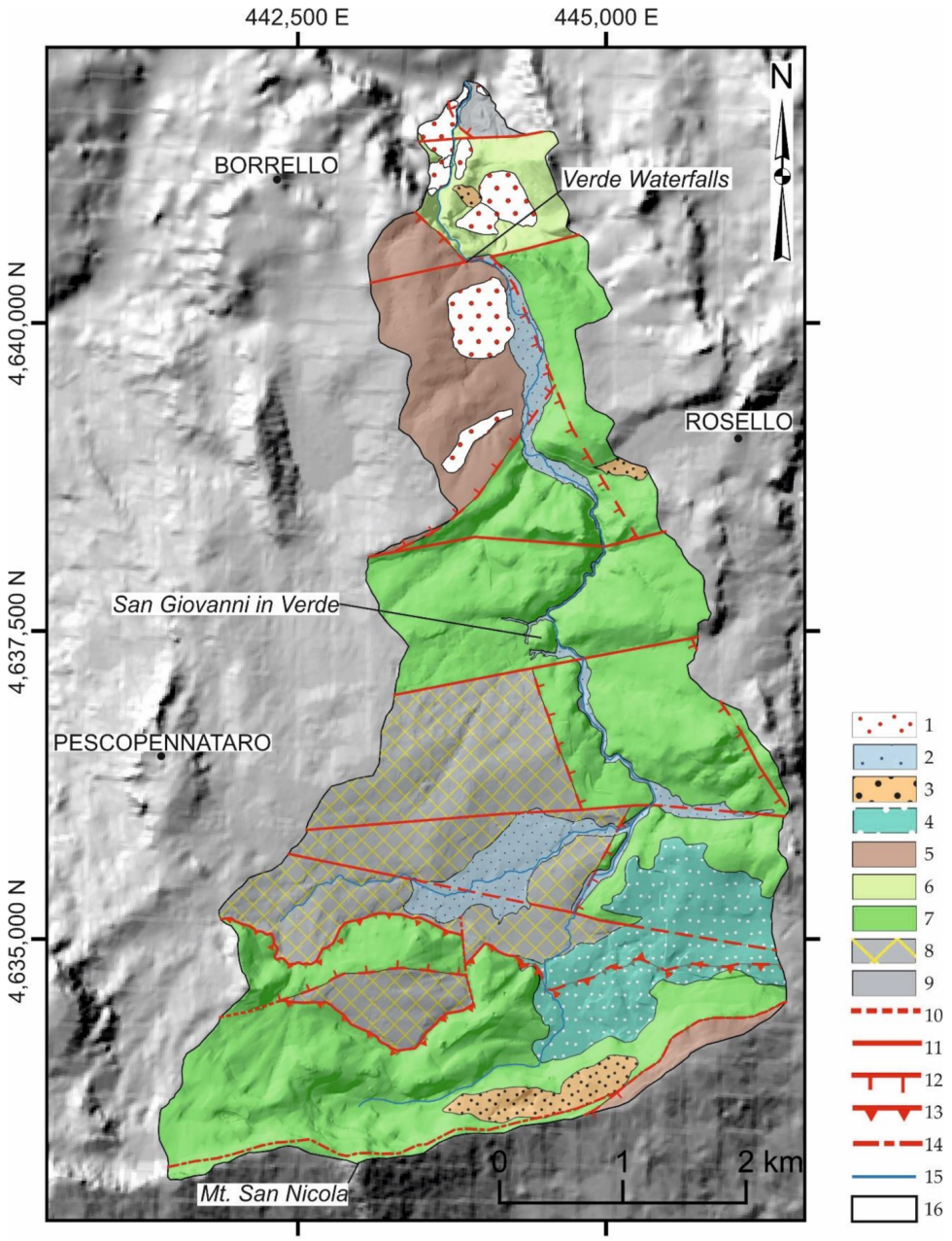

Figure 5. Geological scheme of the study area. Legend: (1) landslide deposits (Holocene); (2) fluvial deposits (Holocene); (3) red soils (Holocene); (4) palustrine deposits (Pleistocene–Holocene); (5) pelitic–arenaceous deposits (Late Miocene); (6) calcareous and marly–calcareous deposits (Middle Miocene–Late Miocene); (7) calcarenite and calcirudite deposits (Middle Miocene); (8) calcarenitic deposits (Late Cretaceous–Early Miocene); (9) clay deposits (Late Cretaceous–Early Miocene); (10) uncertain trace fault; (11) strike-slip fault (dashed if uncertain or buried); (12) normal fault (dashed if uncertain or buried); (13) thrust (dashed if uncertain or buried); (14) uncertain geometry fault; (15) Verde Stream's main course; (16) watershed boundary.

3. Methods

The Verde Stream was investigated through a drainage basin scale geomorphological analysis incorporating (i) the morphometry of orography and hydrography, (ii) photogeological analysis, and (iii) structural geomorphological field mapping. This analysis was performed using topographic maps

(1:25,000–1:5000 scale) and supported by the use of a 20 m digital terrain model as a base map and by the creation of a digital elevation model (5 m DEM) derived from 1:5000 scale regional technical maps.

Morphometric analysis was carried out in a geographic information system software (QGIS 2016, version 2.18 "Las Palmas"). It was based on the definition of the drainage network of the Verde Stream, hierarchized according to Strahler [66]. The drainage lines were digitized from 1:5000 topographic maps and verified by means of 1:33,000 and 1:10,000 air-photos; first order stream was defined from stereographic image analysis according to the stream channel incision. The main Verde drainage basin was then classified into 16 sub-basins, extracted taking into account those related to the junction of the minor streams (first, second, third order) to the main stream (fourth order) [66,67]. The morphometric analysis is based on four main parameters: slope, energy of relief, hypsometric curves and integral values, erosion index. The slope was calculated as the first derivate of elevation [68–71]. The local relief was calculated as the elevation range within 500 x 500 m windows, according to Ahnert [72]. The hypsometric curves were calculated for each of the sub-basins and for the entire basin and represent the normalized area vs. altitude distribution within the basins [68]. The curves were obtained by plotting the proportion of the total basin height (relative height) against the proportion of total basin area (relative area) [68] and for each curve the hypsometric integral ($\int_{ips}$) was calculated as the area under the curve. The obtained curves were grouped into three main families [68,69,73], each characterized by a different trend (i.e., concave, convex, and planar). The hypsometric curves and values are connected to the degree of dissection of the basin but are also highly controlled by lithology and morphostructural setting. Convex hypsometric curves characterize 'young' weakly eroded basins affected by linear incision and incipient dissection; S-shaped curves are typically associated to intermediate basins with moderate erosion and an already developed dissection; and, finally, highly eroded basins show concave curves [19,20,69,73–75]. This contributed to evaluate the evolutionary stage and dissection of the entire basin and for the characterization of the different sectors of the basin. The erosion index was estimated following a methodology already applied in similar studies in drainage basins of central and southern Italy [76–78]. It was derived by applying empirical equations, which link morphometric parameters (i.e., drainage density, D; and the hierarchical anomaly index, Δa) and the turbidity transport (Tu), expressed in $t/km^2/year$. This analysis was carried out for the entire basin and for the 16 sub-basins. The mathematical equations [76] are

$$\text{Log Tu} = 0.33479\ \text{D} + 0.15733\ \Delta\text{a} + 1.32888, \quad (1)$$

valid in sub-basins with drainage density (D) less than 6, and

$$\text{Log Tu} = 1.44780 + 0.32619\ \text{D} + 0.10247\ \Delta\text{a}, \quad (2)$$

valid in sub-basins with drainage density higher than 6. Therefore, it is possible to convert the obtained Tu into the erosion index (Id), applying a calculation using the specific weight of the outcropping lithologies whose values range between 2.0 and 2.4 kN/m^3, appropriately justified by its mineralogical and geotechnical features.

The drainage network was analyzed focusing on pattern types and the azimuthal distribution of the obtained hierarchical orders was defined [79,80]. The azimuthal distribution rose diagrams were extracted by considering the length of the streams (subdividing them into 50-m-long segments). This allowed us to detect stream orientations that may be controlled by tectonics, as already observed in several morphotectonic studies carried out in the Adriatic piedmont [13,38,81–85]. In particular, the first order streams orientation can be strongly influenced by active morphotectonic processes, whereas the distribution and geometry of higher order streams can be related to a more long-term evolution and to a complex combination of morphogenetic factors.

Geomorphological analysis was based on stereoscopic air-photo interpretation and field mapping. Air-photo interpretation was performed using 1:33,000 and 1:10,000 scale stereoscopic air-photos (Flight GAI 1954 and Flight Abruzzo Region 1981–1987) and 1:5000 scale orthophoto color images.

Combined to the field mapping, it supported the morphotectonic investigation of the study area. Field mapping was carried out at 1:5000 scale, investigating outcropping bedrock lithology, superficial deposits, and different types of landforms (structural, slope, fluvial, and karst). The mapping was performed according to the guidelines of the Geological Survey of Italy and AIGeo [86–89] and in accordance with the literature concerning structural geomorphological mapping [3,89–91]. Concerning the geomorphic evidence of tectonics, the morphotectonic approach originally proposed by Ambrosetti [92] and improved by more recent works [2,3,39,73,81–84,90,93–96] was followed, focusing in particular on elements concerning ridges, slopes, valleys, and hydrography. Moreover, such elements were analyzed concerning the connection with passive or active role of tectonics in the landscape. Some features (e.g., ridges, structural scarps, and saddles) are structural related landforms, while other elements (i.e., river bends, hanging and beheaded valleys, 90° confluence) can be considered as morphological evidence connected to the active role of tectonics. All the possible alignments of the main features were defined considering the connection of landforms along specific orientations, also through interpretation of air-photo and DEM-derived shaded relief images. Their azimuthal distribution was determined and extracted by considering the frequency of the landforms. The connection and alignment of the mapped geomorphological elements along a specific orientation can give evidence of morphotectonic processes and suggest the passive or active role of tectonics in the landscape shaping and can therefore be indicative of Quaternary tectonic deformations [13,38,80–83]. The tectonic origin of these alignments was verified by combining the geomorphological observation with all the available geological knowledge and through geomorphological sections. The analysis of the morphotectonic alignments and the realization of geomorphological sections allowed to combine and discuss all the gathered data and to outline the main systems of tectonic discontinuity.

Finally, the results of the local investigations in the Verde Stream catchment area were integrated with the analysis of the junction area with the Sangro River and with the analysis of the Sangro's long profile compared with previous work in the inner mountain area and in the piedmont area. This analysis outlined the distribution of karst landforms and hanging landscapes in the middle Sangro River valley and these features were compared to the montane and piedmont fluvial terraces through the long profile in order to outline the main steps of the landscape evolution of this area [2,12,34].

4. Results

4.1. Orography and Hydrography

The Verde Stream catchment area reaches its maximum altitude on the ridge Mt. San Nicola (1517 m a.s.l.)–Mt. Campo (1640 m a.s.l.), along the southern divide, while to the north the topography slopes down gradually, then drops down with sharp scarps to a minimum of 420 m a.s.l. at the confluence with the Sangro River. Based on the orography of the landscape (elevation, slope, energy of reliefs), the study area can be subdivided into three different sectors. The southern sector (I, in Figure 6) is a mountain area characterized by a wavy and irregular morphology. The orography is dominated by the ridge featuring the southern watershed of the basin (maximum altitude of about 1500–1600 m a.s.l.). It shows a homogeneous slope distribution (values between 55% and 150%). The southern ridge features higher values (>150%), while northern flat areas show values <20%. The energy of relief ranges from 2 m to 300 m, with the highest values along the northern escarpment of Mt. San Nicola. The central sector (II, in Figure 6) is an intermediate wavy upland at an elevation from 750 to 1000 m a.s.l., with some local steep slopes to vertical scarps along the northern edge of the upland area. Slope values range from 15% to 55%, and the energy of relief ranges from 60 m to 180 m. The transition to the northern sector (III, in Figure 6) is marked by a wide sharp scarp on which the Verde Waterfalls are located. The elevation drops from 700 and 420 m a.s.l. moving toward the Verde Stream–Sangro River junction. Slope values are >100% and the energy of relief ranges from 180 m to >300 m, with the highest values along the vertical scarps of the waterfalls.

The Verde Stream drainage basin has a 22.72 km^2 area and is divided into 16 sub-basins that cover an area of 19.21 km^2; the remainder is made up of interfluve areas. The drainage network shows a mainly sub-dendritic drainage pattern in the northern sector, which is connected to clayey bedrock lithology and a generally angular one in the central and southern sectors, related the structural control of the faulted carbonate bedrock. At the transition between central and northern section, a sharp knick zone defines the Verde Waterfalls with a triple 200 m high jump (the highest natural waterfalls of Italy). The hierarchized drainage network shows four orders (according to Strahler [66], Figure 7): the first order streams show a main E–W trend and a minor SW–NE one; the second order streams are mainly arranged in the SW–NE direction (with minor E–W ones); the third order streams are mainly along the SSW–NNE and WSW–ENE directions; and, finally, the fourth order streams show preferential SSE–NNW and S–N orientations (Figure 7). This analysis outlines a "rotation" in the azimuth arrangement of the streams from the first to the fourth order, from E–W to S–N and SSE–NNW.

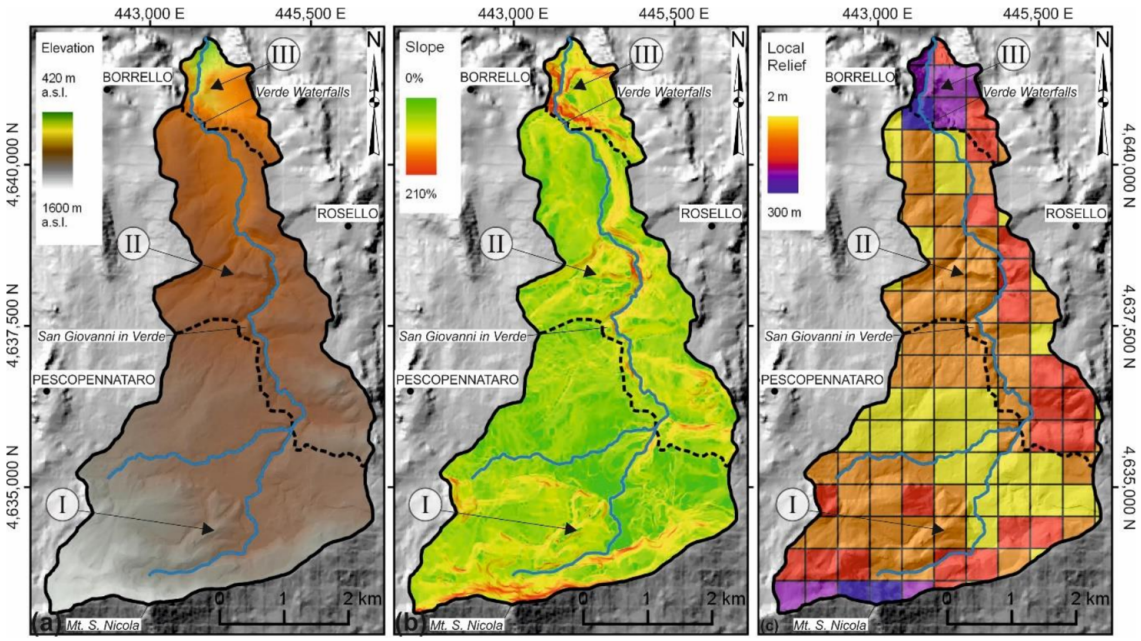

Figure 6. Physiographic features of the study area: (**a**) elevation map; (**b**) slope map; (**c**) local relief map. The dashed black line indicates the orographic sector boundary (numbers I, II, III); the blue line, the main course of the Verde Stream; the black line, the watershed boundary.

4.2. Hypsometric Curves and Integral

Basins with concave hypsometric curves occur mostly in the southern Verde area at the highest elevations and close to the southern ridges, and hypsometric integrals show low values ($\int_{ips} < 0.45$). The central sector is characterized by markedly convex curves (except for a couple of concave curves at the transition with the southern slope). The values of the hypsometric integral range from high to very high ($0.55 < \int_{ips} < 0.80$). The northern sector show S-shape curves with intermediate integral values ($0.45 < \int_{ips} < 0.50$). This peculiar setting (Figure 8) outlines an intermediate erosion stage with large dissection in the northern sector of the basin close to the junction with the Sangro River and, as expected, downstream from the Verde Waterfalls. Poor erosion with prevailing linear erosion characterizes the intermediate sector outlining an incipient dissection. The southern sector is hanging at the highest elevation, dominated by areal erosion and not affected by dissection except for a single basin at the transition with central sector.

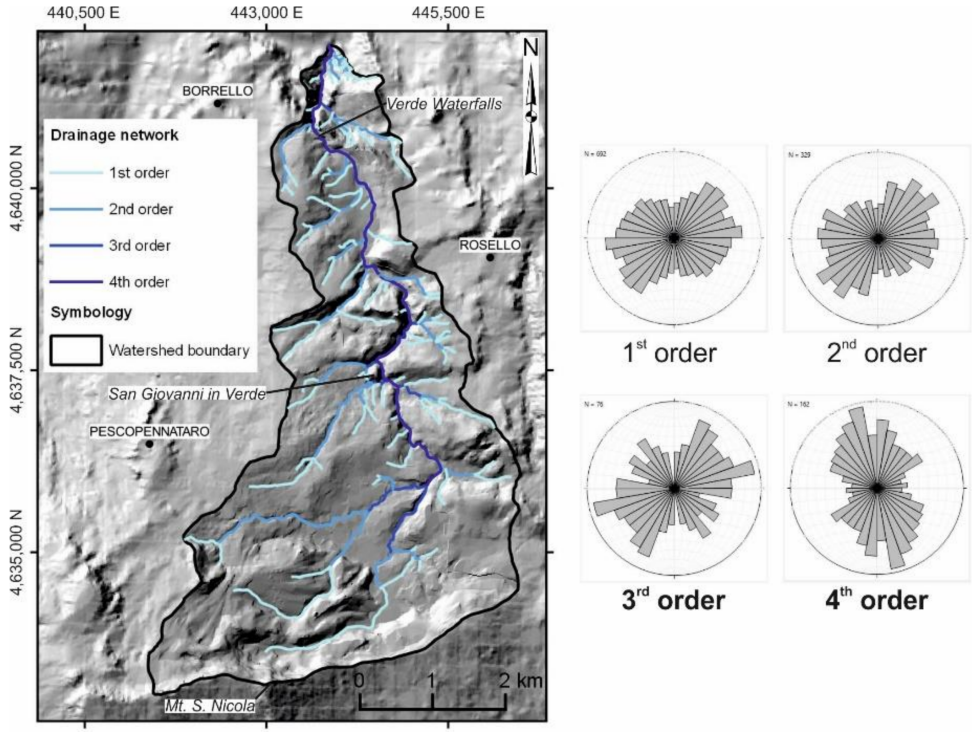

Figure 7. Drainage network divided into hierarchical orders (according to Strahler [65]) and drainage lines azimuth distribution for each order.

4.3. Erosion Index

Basins with low values occur mostly in the southern sector at the highest elevations and close to the southern ridges. The values of the erosion index tend to increase progressively moving towards the north, so that the central sector is characterized by intermediate values. The northern sector shows the highest values. This peculiar setting (Figure 9) outlines a high erosion index (Id > 0.56) with large dissection in the northern sector of the basin close to the junction with the Sangro River and, as expected, downstream from the Verde Waterfalls. An intermediate erosion index (0.1 < Id < 0.4) with prevailing linear erosion characterize the intermediate sector outlining an incipient dissection. The southern sector is dominated by areal erosion with a low erosion index (Id < 0.11).

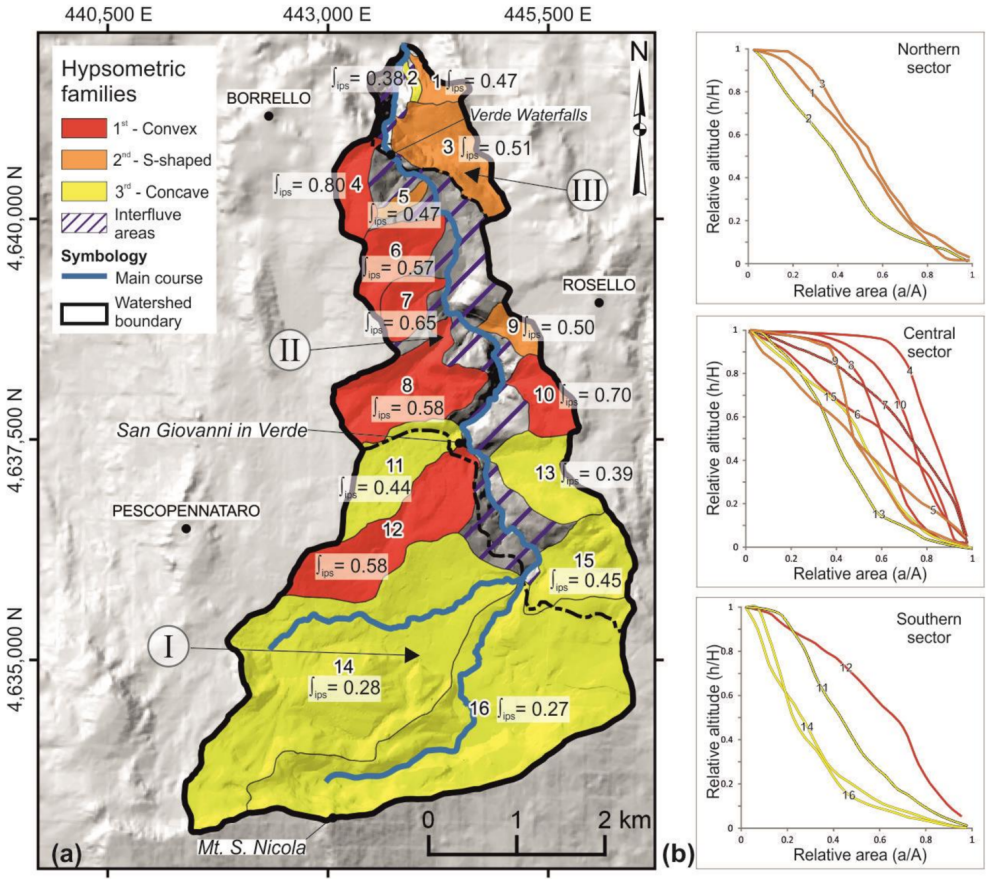

Figure 8. (**a**) Hypsometric families map (numbers refer to the drainage sub-basin). The dashed black line indicates the orographic sector boundary (numbers I, II, III). (**b**) Hypsometric curves of each orographic sector; in red: convex shaped curves belong to the first hypsometric family; in orange: S-shaped curves belong to the second hypsometric family; in yellow: concave shaped curves belong to the third hypsometric family.

4.4. Geomorphological Analysis

The most recurrent features are fluvial and slope gravity landforms (Figure 10a), as well as structural related landforms and evidence of tectonics, which underwent a specific investigation (Figure 10b). In detail, in the southern sector, soil creep is widespread in areas with low gradients and involve calcarenitic and palustrine deposits. Fluvial landforms are represented by concave valleys and gullies near the escarpment of the southern watershed (Mt. San Nicola) and by flat bottom valleys on areas characterized by medium–low gradients. These features outline prevailing areal erosion in this sector. The central sector is characterized by rotational slides, which involve pelitic–arenaceous deposits. Fluvial erosion scarps laterally confine the channels of the Verde Stream with an altitude ranging from a few meters to ~10 m. Gullies and V-shaped valleys are widespread and deeply incised in calcarenite and calcirudite deposits near San Giovanni in Verde. These elements indicate an incipient dissection and landscape rearrangement. Finally, the northern sector features the most relevant landslides mainly consisting of rockfalls, that evolve into topples, and become earthflows in the lower part of the slope. Falls are widespread near the Verde Waterfalls along vertical or steep slopes on calcareous and marly–calcareous deposits. Separation occurs along discontinuities such as fractures, joints and bedding planes, and movement occurs by free-fall, bouncing and rolling. Flows, instead, involve clay deposits outcropping near the Verde Stream–Sangro River junction. Furthermore, the sector is affected by a deep-seated gravitational slope deformation (DSGSD) that magnifies its geomorphological instability. The mapped fluvial landforms include fluvial erosion scarps, gullies,

badland areas, V-shaped, and asymmetric valleys and hanging valleys. The waterfalls and a large badland area represent the most important fluvial landforms, both located in the northernmost portion of the area. These features indicate the strong dissection occurred in the area in terms of fluvial incision and landsliding.

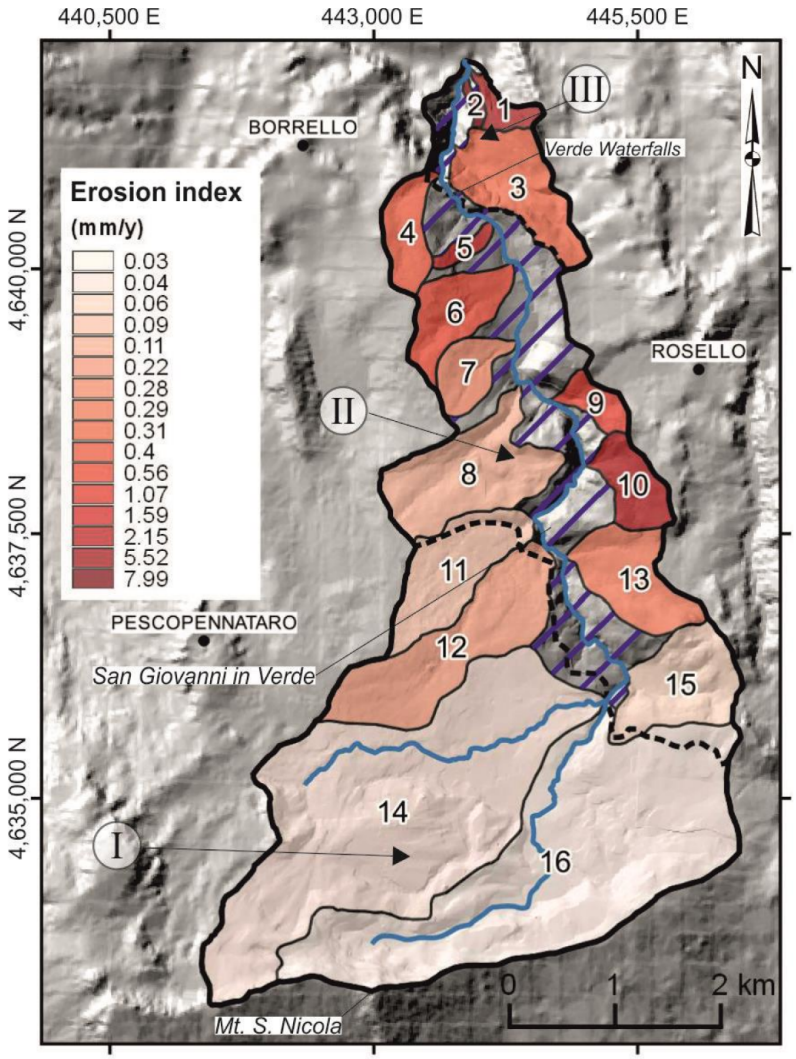

Figure 9. Erosion index map (numbers refer to the drainage sub-basin). The dashed black line indicates the orographic sector boundary (numbers I, II, III); the blue line, the main course of the Verde Stream; the black line, the watershed boundary.

The structure related landforms and the morphological evidence of tectonics (valleys, ridges and hydrography) were also investigated in detail (Figure 10b) and the most significant elements show a peculiar distribution and orientation in the main sectors of the valley. The southern sector is mostly dominated by structure related landforms which outlines a passive control of the tectonic structures. Straight symmetric and asymmetric ridges are found along the southern watershed with a preferential ~N75°E orientation (the western segment is symmetrical, while the eastern one, with the northern slope steeper than the southern one).

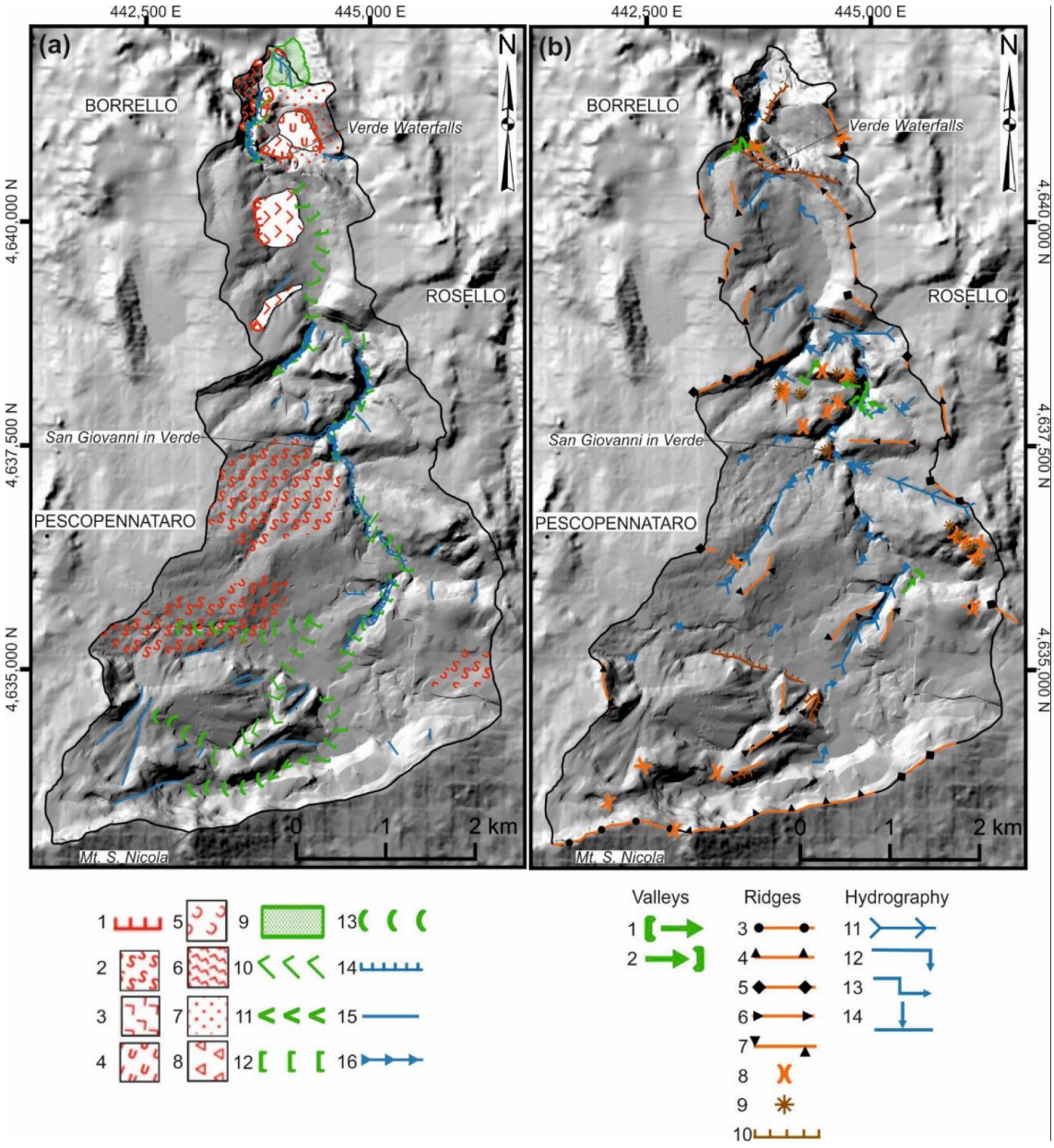

Figure 10. (**a**) Map of the fluvial and slope gravity landforms. In black: the watershed boundary. Legend: (1) degradational and/or landslide scarp; (2) soil creep; (3) rotational slide; (4) translational slide; (5) earthflow; (6) complex landslide; (7) deep-seated gravitational slope deformation (DSGSD); (8) rockfall; (9) badlands area; (10) asymmetric valley; (11) V-shaped valley; (12) flat bottom valley; (13) concave valley; (14) fluvial erosion scarp; (15) gully; (16) entrenched fluvial segment. (**b**) Morphotectonic scheme. In black: the watershed boundary. Legend: (1) beheaded valley; (2) hanging valley; (3) straight symmetric ridge; (4) straight asymmetric ridge; (5) ridge; (6) altimetric discontinuities of ridge; (7) planimetric discontinuities of ridge; (8) saddle; (9) isolated relief; (10) structural scarp; (11) rectilinear fluvial segment; (12) river bend; (13) double river bend; (14) 90° confluence.

Other ridges and the altimetric and planimetric discontinuities of the ridges show a NNW–SSE trend. Several saddles are distributed mostly on a NNE–SSW direction. Asymmetric valleys feature a SSE–NNW trend. Rectilinear fluvial segments are found with a NE–SW trend. River bends show a prevalent direction from N–S to NE–SW. In the central sector both structure related landforms and evidence of tectonics are present. The former consist of, V-shaped valleys (mostly in NE–SW and in NW–SE directions), asymmetric valleys (NE–SW direction), ridges and the altimetric-planimetric

discontinuities of ridges (from about N–S to E–W), isolated reliefs and saddles (widespread and mostly in NW–SE direction). The evidence of tectonic are mostly related to rectilinear fluvial segment (in a NE–SW direction), river bends (main orientation from N–S to NE–SW, with a large number of alignments in the NNW–SSE direction), 90° confluence (along NE–SW and NW–SE prevalent directions), and particularly hanging and behaded valleys (mostly on WNW–ESE and SW–NE orientation). In the northern sector, V-shaped and asymmetric valleys extend in N–S to NE–SW directions. Ridges and the altimetric and planimetric discontinuities of ridges present a trend from N–S to NE–SW; the isolated reliefs are distributed in the NNW–SSE direction. River bends show a prevalent direction from E–W to N–S.

5. Discussion

5.1. Morphometric Features

The distribution of the morphometric features outlines the different characteristics of the orographic sectors, also compared to the landform distribution. In particular, the southern sector shows a gentle landscape, with low values in slope and energy of relief and concave hypsometric curve (low value of $\int_{ips}$); in this sector, areal erosion landforms prevail, probably linked to an old phase of modeling of the landscape. The central sector shows an incipient dissection of the landscape, outlined by convex hypsometric curve (high values of $\int_{ips}$) and confirmed by the presence of deep V-shaped valleys and entrenched fluvial segment with high values of slope nearby the valleys. The northern sector is strongly dissected and eroded as testify by very high values in slope and energy of relief and by the presence of many landslides. This analysis outlines the possible evolution of the landscape, which is in state of progressive dissection from N to S; the dissection has only partially reached the central sector, while it has not reached yet the southern one.

5.2. Morphotectonic Features

The morphological field evidence of tectonics deduced from the geomorphological features of valleys, ridges, and hydrography was analyzed in detail. The alignments of these landforms were investigated and provide a geomorphological contribution to the morphotectonic reconstruction of the area and significant indications of Quaternary tectonic deformations. From the type of landforms (related to morphotectonics or selective erosion), their distribution and preferential orientation, we outlined some alignments mainly with NE–SW, E–W, and NW–SE trends. The data concerning the azimuthal analysis of the drainage network (Figure 7), anomalies in lithological contacts (Figure 5), geomorphological field mapping (Figure 10), and alignments of morphological evidences of tectonics (Figure 11) allowed us to define different tectonic alignments (Figure 12). They can be distinguished into four families:

- S1: interpreted as a thrust with E–W trend;
- F1: oriented NE–SW;
- F2: with a trend variable from NNW–SSE to NNE–SSW;
- F3: oriented in the E–W and ENE–WSW direction.

In particular, the S1, F1, and F2 families seem to be connected to structural landforms (i.e.,ridge, saddles, isolated reliefs), while the F3 family appears linked to morphological evidence of tectonics (i.e., river bends, hanging and beheaded valleys, 90° confluences). On this basis we can deduce that the tectonic features belonging to the F3 family acted in more recent time than the other tectonic feature. In accordance with other authors [26–28], the age of compressive movement (S1) can be referred to Upper Miocene–Lower Pliocene; F1 and F2 are poorly constrained to Pliocene and Lower Pleistocene; as results from this study the F3 (from E–W to ENE–WSW) is the youngest tectonic features and is interpreted as a left-lateral strike-slip fault system aged in the Middle-Upper Pleistocene.

Moreover, the surface morphotectonic evidence can be confirmed by the recent seismicity occurred after the geomorphological investigation from April to August 2018 that outlines recent activity of E–W deep tectonic structures in the Molise area. This is also supported by more eastern tectonic structures responsible for historical and recent earthquakes connected to E–W structures (e.g., 1627 Mw 6.8; 2012 Mw 5.72 [6–8]) (Figure 13).

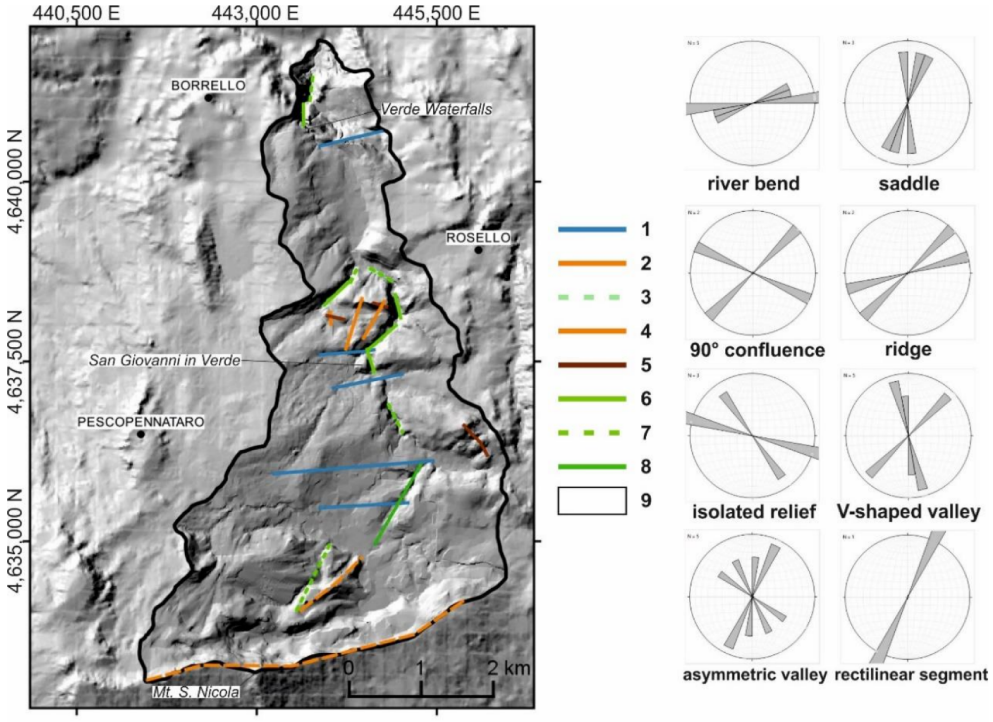

Figure 11. Alignment schema of morphotectonic elements and azimuth distribution of the alignments. Legend: (1) alignment of river bends; (2) alignment of saddles; (3) alignment of 90°confluence; (4) alignments of ridges; (5) alignment of isolated reliefs; (6) alignment of V-shaped valleys; (7) alignment of asymmetric valleys; (8) alignment of rectilinear fluvial segment; (9) watershed boundary.

5.3. Geomorphological Domains

According to the morphometric, geological and geomorphological features, the different orographic sectors, thoroughly discussed in the previous section (Figures 6–9), correspond to three geomorphological domains, with different morphotectonic and morphosculptural elements. Their arrangement is summarized in Table 1 and graphically shown in Figure 14.

Table 1. Geomorphological domains of Verde Stream catchment area

Geomorphological Domain	Orography (m a.s.l.)	Slope (%)	$\int_{ips}$	Local Relief (m)	Slope Gravity Processes (Landforms)	Fluvial Processes (Landforms)
Southern	1600–1000	55–210 0–20	<0.45	2–18 0~300	Slow down-slope movement (soil creep)	Limited river erosion (flat bottom and concave valleys)
Central	1000–750	15–55	$0.55 < \int_{ips} < 0.80$	60–180	Slow down-slope movement (Soil creep)	Linear downcutting (V-shaped valleys)
Northern	750–420	> 100	$0.45 < \int_{ips} < 0.50$	180–300	Landslides (rockfalls, topples, DSGSD)	Areal erosion (badlands area); linear river erosion (gorge, waterfalls)

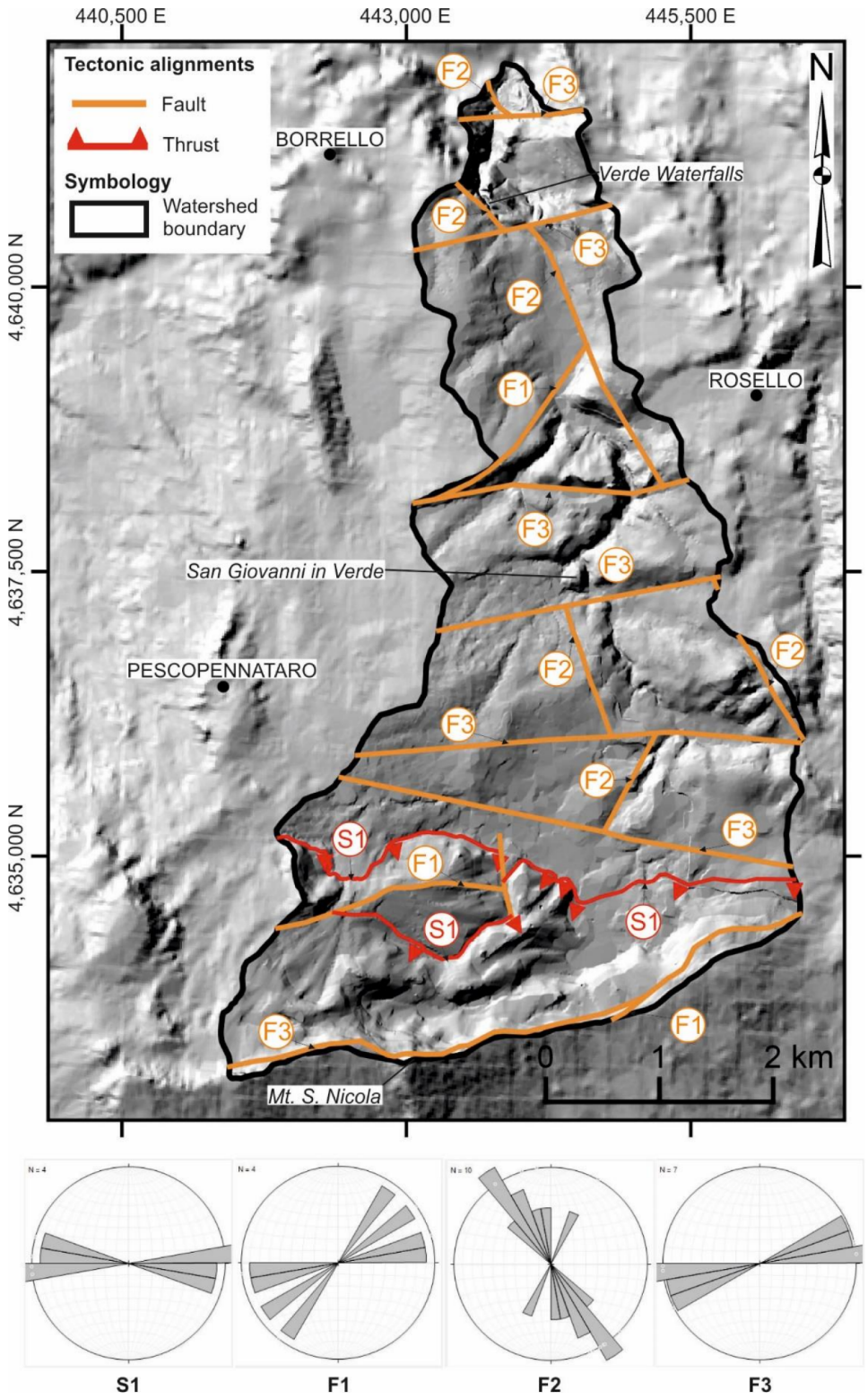

Figure 12. Morphotectonic scheme showing tectonic features, the relevant azimuthal distributions, and the different phases.

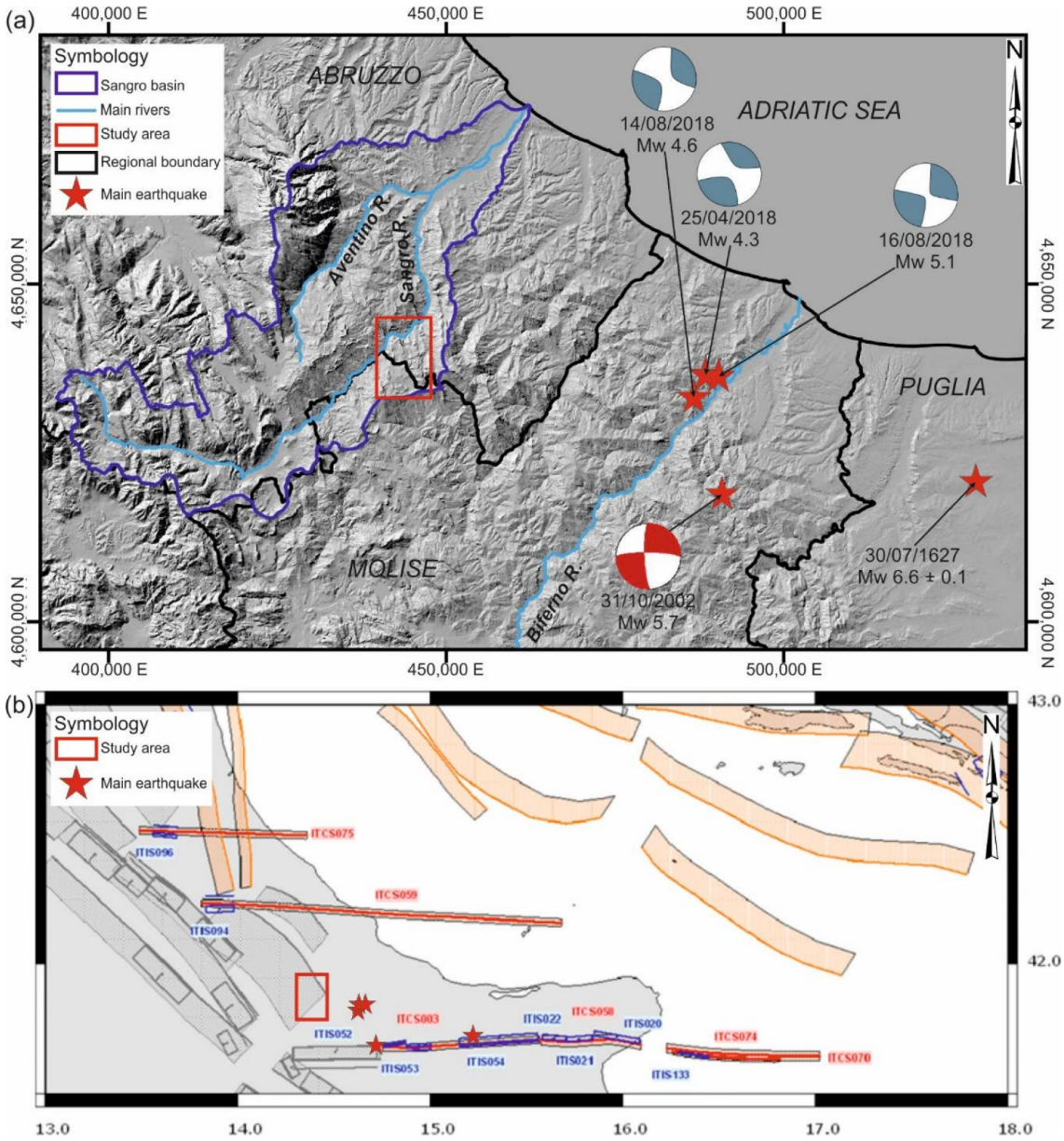

Figure 13. (**a**) Historical and recent earthquakes near the study area, connected to E–W structures, as indicated by focal mechanism. (**b**) E–W deep tectonic structure near the study area and recent earthquakes (modified from [6]).

The morphotectonic setting, defined by the tectonic families (Figure 12), is modified by the development of surface processes determining the morphosculptural architecture of the study area and a significant difference in the morphological setting. This dynamic and mutual interaction allowed us to characterize the different geomorphological domains from a morphogenetic standpoint and to identify:

- the development of landforms and processes due to the drainage network incision, resulting from a combination of both areal denudation (badland area) and linear downcutting (V-shaped valley, widely present in the central geomorphological domain);
- the development of slope processes and landforms due to slope gravity areal denudation, widely present in the northern geomorphological domain near the Verde Waterfalls.

The southern sector shows a subdivision into two sub-sectors, divided by a thrust structure with a E–W trend: the first one is represented by a mountain area with the highest elevations close to the southern ridges where structural landforms, like ridge and saddles, prevail; the second one is characterized by a wavy and irregular morphology in which prevail slow down-slope movement and limited river erosion; in the entire northern sector morphosculptural processes are widespread.

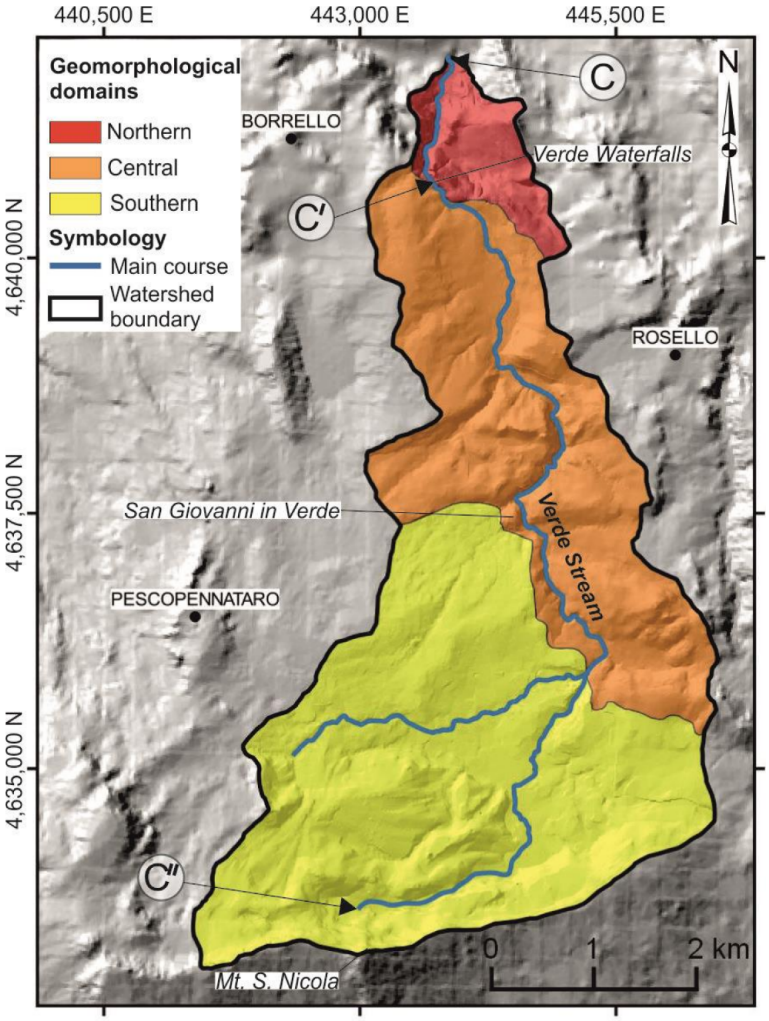

Figure 14. Geomorphological domains of the study area, on which different morphosculptural processes took place (location of letters C, C′, C″ in Figure 1).

The central sector is dominated by linear down-cutting, which creates an incipient dissection in the steep V-shaped valleys around the wavy upland. The morphotectonic framework of this sector is mostly influenced and controlled by the elements with an E–W trend. The northern sector is characterized by fluvial processes with a predominance of areal erosion in the badlands area and linear erosion in the gorge downstream of the waterfalls (as testify by the presence of asymmetric and V-shaped valleys and by entrenched fluvial segment). This area is also affected by a geomorphological instability outlined by slope gravity processes, among which is possible to highlight rockfalls, topples and a DSGDS.

The geomorphological section (Figure 15) shows the clear morphological difference between the southern-central and the northern geomorphological domains, divided by the waterfalls. Therefore, the Verde Waterfalls become a key morphological element that marks the boundary between two landscapes, which are different in terms of their geological and geomorphological features. In the southern-central domains, an old, hanging, and weakly-undulating landscape, still

preserved by river incision, can be observed; while, the northern domain, moving towards the Verde Stream–Sangro River junction, features a young, active and dynamic landscape marked by significant geomorphological instability.

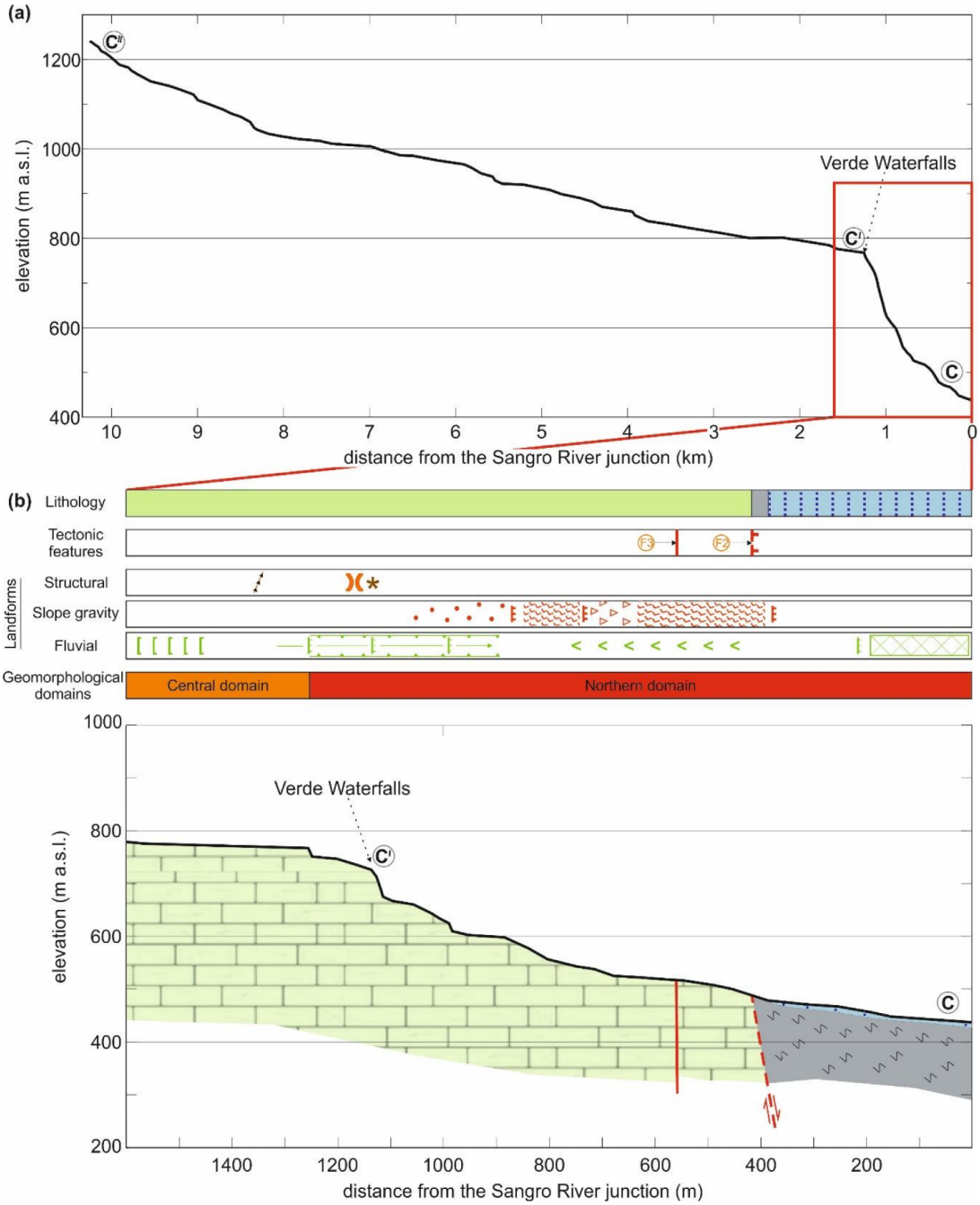

Figure 15. (**a**) The Verde Stream's long profile; (**b**) geomorphological section of the northern reach of the Verde Stream's long profile (red box); location in Figures 1–14 (letters C, C′, C″).

5.4. Karst Features and Paleo-Landscapes

The karst morphogenesis is a widely developed process in the Central Apennines chain and may represent a key element in understanding the landscape evolution of the study area. Usually, this aspect is underestimated in several works that focused on Quaternary fluvial geomorphological analysis. For this reason, the results of the morphotectonic and geomorphological analysis were compared with the distribution of the karst features found near the Verde Waterfalls and represented

by several small doline and a large broken doline (Figures 16 and 17), located at an altitude from 580 to 780 m a.s.l. Therefore, the Verde Stream catchment area is connected to karst features and can be considered as a karst groundwater system with perennial flows rate observable in the waterfalls area [65].

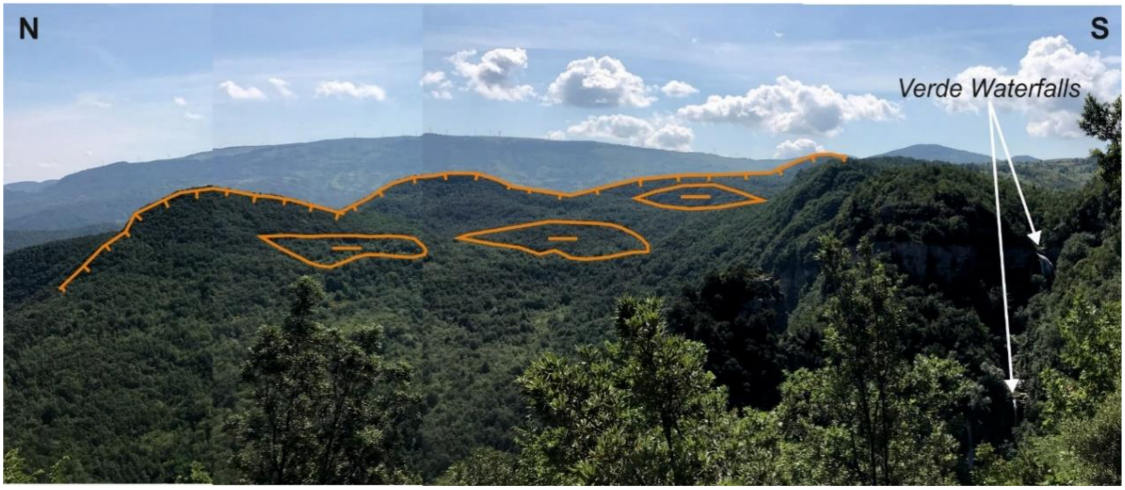

Figure 16. Broken doline near the Verde Waterfalls (780–580 m a.s.l.).

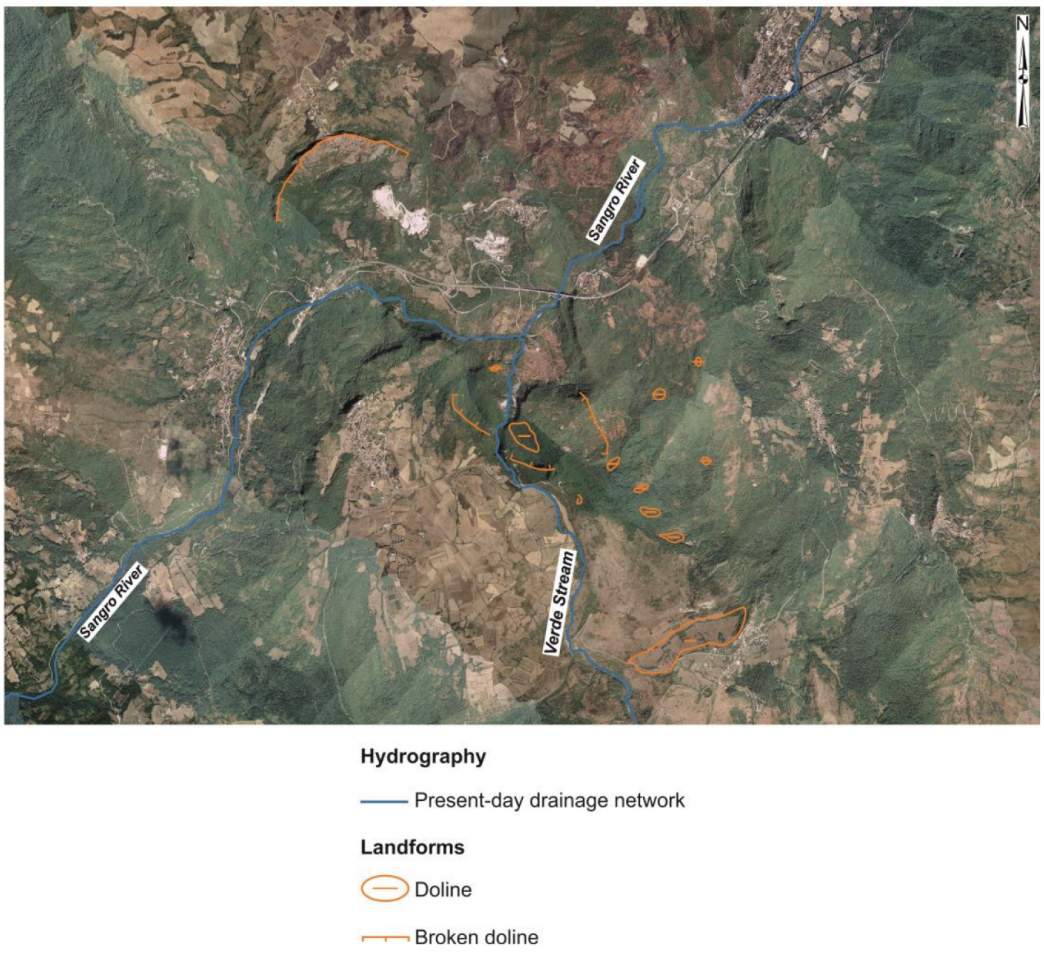

Figure 17. General framework of karst landforms in the Verde Stream–Sangro River junction area (provided by Abruzzo Region ortophotos).

According to the geomorphological framework of the Verde Stream catchment area, characterized by a clear landscape difference in between the southern-central and the northern geomorphological domains, this morphological setting together with the karst features was investigated in the Verde Stream–Sangro River junction area (Figure 17) and in all the middle Sangro River valley. Karst landforms are widespread at an altitude ranging from 500 to 900 m a.s.l., while gently undulating landscapes, preserved as relict paleo-landscape (Figure 18), are developed, with an altitude from 850 to 1000 m a.s.l., close or at the present drainage divides.

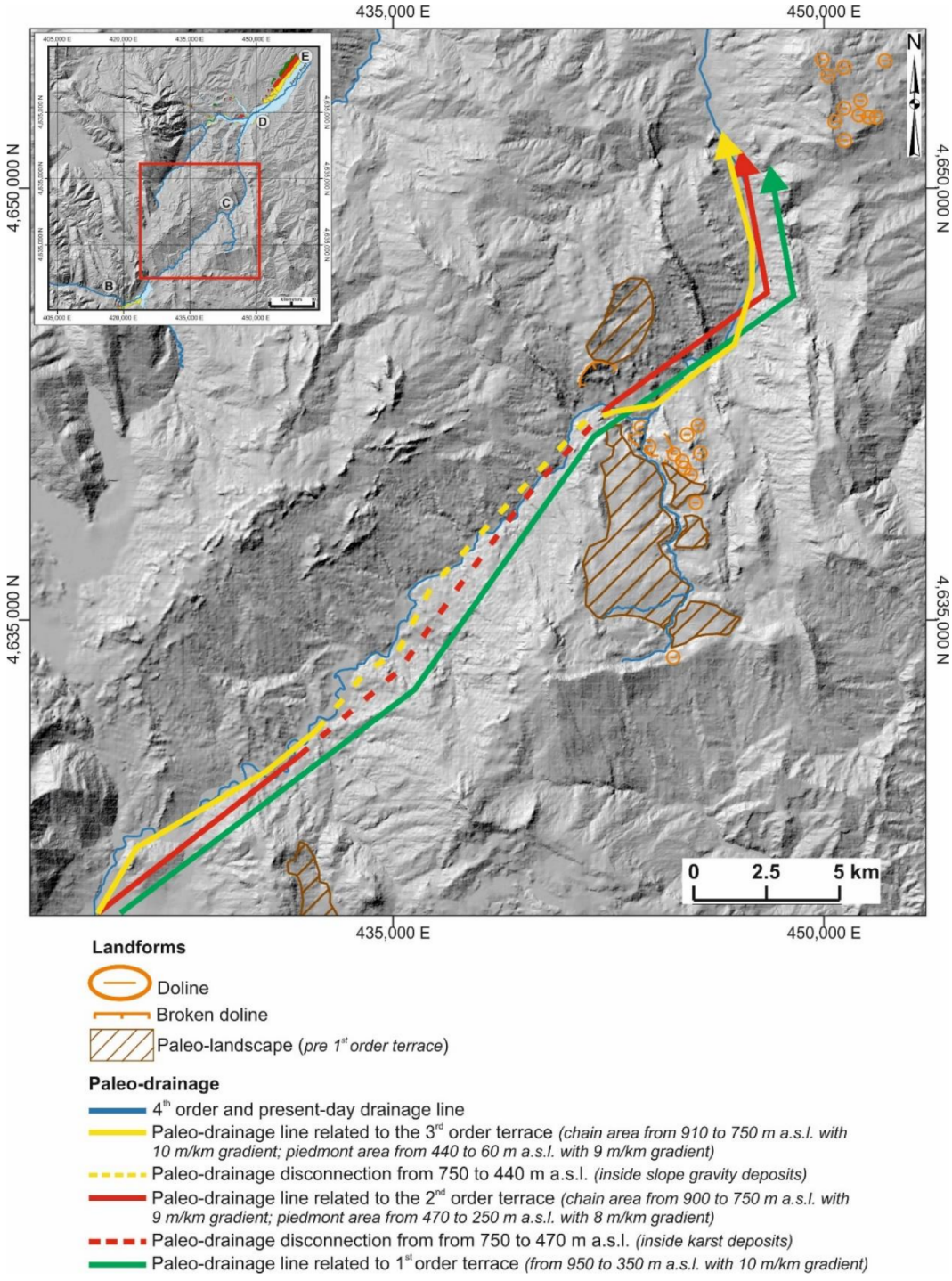

Figure 18. Possible paleo-drainage of the Sangro River at different stages. The top left shows Figure 3, to which the colors and age of the paleo-drainage refer.

To investigate the study area in the general framework of the middle Sangro River (Figure 18), the results of the geomorphological analysis were compared with the elevation's distribution of paleo-landscapes, karst landforms, and fluvial terraces along the Sangro River's long profile (Figure 19). On the profile the main paleo-landscapes and karst landforms were projected, each with its own relative elevation above the present course, pointing out the key role of karst morphogenesis. This comparison outlines the presence of paleo-surfaces with an altitude ranging from 850 to 1000 m a.s.l. and the clustering of karst landforms at certain altitudes (500–900 m a.s.l.).

The southern-central sectors of the Verde Stream catchment area correspond to one of these relict paleo-landscapes and is dissected by karst landforms. The main scarp dividend the northern and the southern-central sectors shows a semicircular trend and can be interpreted as a large broken doline, which evolved due to gravity-induced and fluvial processes. Similar features were observed on the northern side of the Sangro River, where a large gently wavy landscape is dissected by a semicircular scarp, again defined as remnant of a large doline features broken by gravity induced processes. Paleo-landscape features are also present in the southern side of the Sangro River and also in the northern one (Figure 18) at elevation ranging from 400 to 100 m a.s.l. (Figure 19). The result of this analysis outlines a possible hanging karst paleo-landscape that can be considered as a remnant of ancient landscapes, which developed at the beginning of the general evolution of the area, before drainage incision, aged at least pre-Middle Pleistocene.

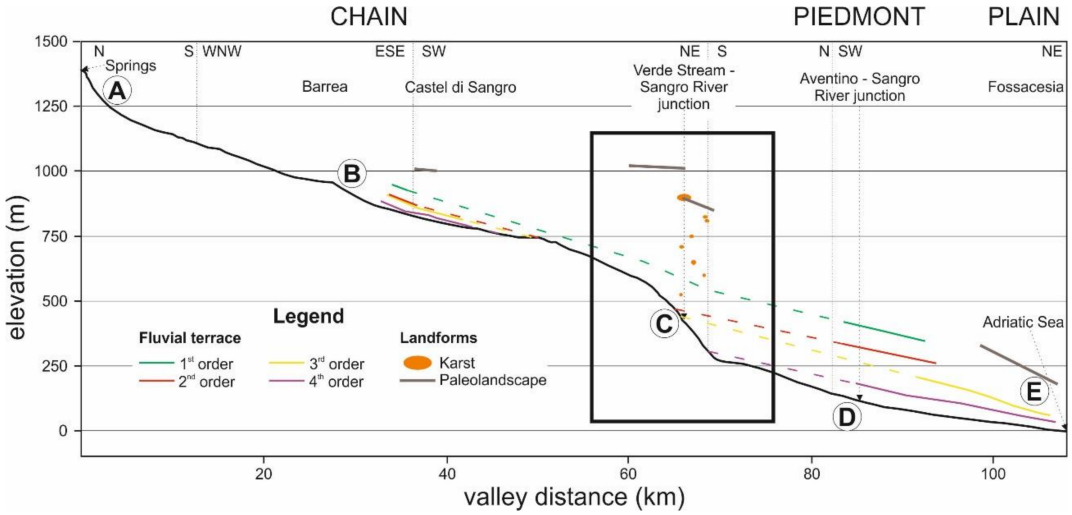

Figure 19. The Sangro River's long profile with the plot of the karst landforms and the terraces gradient found in the Castel di Sangro plain [12,34] and those found in the plain near the Aventino–Sangro River junction [2]. The ages of these deposits are first order terrace, Middle Pleistocene; second order terrace, Late–Middle Pleistocene; third order terrace, Late Pleistocene; and fourth order terrace, Holocene [2]. Location of the study area (box); location in Figure 1, Figure 3, and Figure 14 (letters A, B, C, D, E).

6. Conclusions

The morphotectonic investigation presented in this paper allowed us to outline the role of paleo-drainage, morphotectonics, and surface processes in landscape evolution of the Verde Stream catchment area and middle Sangro River valley (Central Italy). This area is located in the transition zone between Apennines chain and piedmont area and features a complex geological setting—different types of lithological sequences and tectonic directions—and a recent evolution driven by tectonic processes since the Miocene and by uplift and geomorphological processes post-Early Pleistocene (see also [1–3,13,40,43,79,84,97,98]). The local data obtained from the geomorphological and morphotectonic analysis of the Verde Stream catchment area were compared with the analysis of the middle Sangro River valley and the tectonics and seismicity features of the Abruzzo–Molise area. This provided some relevant clues for the understanding of the geological and geomorphological

features of the boundary zone between the Abruzzo carbonate domain and the Molise allochthonous domain in the Apennines chain–piedmont transition zone.

The Verde area features a hanging landscape (southern and central sectors) deeply incised in the northern part, with the formation of the Verde Waterfall. This is due to the deepening of the Sangro River valley in connection with the dissection of karst features and paleo-landscapes. Four main families of tectonic discontinuities control the geomorphological evolution of the area. S1 (E–W-trending connected to Late Miocene–Early Pliocene thrusts), F1 and F2 (NW–SE-trending high angle faults and NNW–SSE/NNE–SSW-trending faults poorly constrained to Pliocene and Lower Pleistocene) are connected to morphoscultural elements confirming the passive role in the landscape shaping of these tectonic elements. The F3 family (from E–W to ENE–WSW-trending) shows an active role in the landscape shaping particularly evident in the central sector of the Verde area outlined by morphological evidence of tectonics (e.g., river bends, beheaded and hanging valleys, rectilinear fluvial segments, etc.). If this is compared to the regional setting, the surface geomorphological investigation carried out in this work confirms the role of E–W tectonic structures, which are connected to the historical and recent seismicity. This is also confirmed by the focal mechanism of earthquakes occurred in 2002 and in 2018 after the geomorphological investigations and even during the last stage of this paper (i.e., August 2018).

The long profile of the Sangro River valley (Figure 19) outlines the distribution of paleo-landscapes, karst landforms, and (chain and piedmont) fluvial terraces. It shows a marked knick convex zone in the middle part, which is to be related to the combination of regional uplift and lithological control along the profile, rather than thrusting that was not active since the Late Pliocene. The distribution of landscape features along the profile suggests that major karst landforms are remnants of ancient landscapes (at least pre-Middle Pleistocene) that developed at the beginning of the chain landscape evolution (before regional uplift, local tectonic subsidence and drainage systems incision). Moreover, the lacking of fluvial terraces in the middle Sangro valley led us to infer the origin of the connection or disconnection of fluvial terrace with same origin (as climatic terraces) and the age, between chain terraces (in the Castel di Sangro plain [12,34]) and the piedmont ones (downstream the Aventino–Sangro River junction [2]). The long profile shows that only the first order of terraced deposits can be correlated and projected above the present valley profile (assuming a roughly constant gradient of about 10 m/km). The following terrace orders (second to fourth) were projected from the piedmont and the chain area; however, they are disconnected along the marked knick convex zone of the Sangro valley. For this reason and due to the occurrence of hanging karst features, connected to or incising the paleo-landscapes, as well as large landslides, along the present valley sides-bottom [99], the disconnection can be related to karst underground drainage during Middle Pleistocene (second order of terrace) and possibly to landslides during late Middle Pleistocene (third order). Since Late Pleistocene the Sangro River progressively acquired the present arrangement.

The geomorphological evolution of this sector of the Apennine chain–piedmont transition zone, driven by uplift and local tectonics and due to a combination of fluvial, karst and landslide processes, can be summarized in different stages:

- an initial paleo-landscape, with widespread karst landforms, plotted above the first order terrace's projection, aged at least pre-Middle Pleistocene; this landscape is affected by NE–SW and NNW–SSE/NNE–SSW tectonic features (F1–F2);
- dissection of the hanging karst paleo-landscape (as testified by hanging and broken dolines and karst landforms) and development of a paleo-drainage level linked to the projection of first order terraces (Middle Pleistocene); this is driven by uplift and possibly by E–W tectonic features (F3);
- further progressive incision of the middle Sangro valley across the transition zone between Apennines chain and piedmont; creation of the abrupt knick convex zone of the Sangro valley and dissection of the northern sector of the Verde Stream due to karst landscape dissection and slope gravity-induced processes; development of a paleo-drainage level related to second and third

order terraces (late Middle Pleistocene–Late Pleistocene) disconnected in the middle Sangro valley due to karst underground drainage and possibly landslide by paleo-landslide and karst deposits.

Finally, the present-day landscape and drainage network configuration are progressively acquired. The final scenario, still clearly out of equilibrium, is now mostly connected to the dynamic interaction of morphotectonics (uplift E–W tectonic elements, F3) and surface (morphosculptural) processes with a predominance of slope gravity areal denudation and drainage network linear downcutting.

Author Contributions: Conceptualization, E.M. and T.P.; Supervision, Methodology and Data Curation, E.M.; Geomorphological investigation, GIS mapping and Writing—Original Draft Preparation, C.C. and G.P.; Writing—Review & Editing, all the authors.

Funding: This research and APC were funded by Università degli Studi "G. d'Annunzio" di Chieti-Pescara, Miccadei fund.

Acknowledgments: The authors wish to thank the Municipality of Borrello with particular reference Giovanni Antonio Di Nunzio (2016–2018) and Antonio Di Luca (2016–2017), the Natural Reserve of Verde Waterfalls, in particular Dr. Tommaso Pagliani and, finally, the "Rio Verde Ambiente e Turismo snc" with particular reference Giuseppe Di Renzo for the logistical support to the research. They also wish to thank the Cartographic Office of Abruzzo Region by means of the Open Geodata Portal (http://opendata.regione.abruzzo.it/metadata_simple_search/category/108), the Cartographic Office of Molise Region (http://www.geo.regione.molise.it/web/guest/servizio.download) and the IGMI (Istituto Geografico Militare Italiano) for providing the topographic data, aerial photos and orthophotos used for the creation of the 5 m DEM and for the geomorphological investigations. The 90 m SRTM (Shuttle Radar Topography Mission) DEM was provided by NASA (https://www2.jpl.nasa.gov/srtm/cbanddataproducts.html). The authors wish to thank Dr. G. Booth-Rea and the other anonymous reviewers for their critical review of the paper and their precious suggestions, which significantly improved this manuscript.

Conflicts of Interest: The authors declare no conflict of interest.

References

1. D'Alessandro, L.; Miccadei, E.; Piacentini, T. Morphostructural elements of central-eastern Abruzzi: Contributions to the study of the role of tectonics on the morphogenesis of the Apennine chain. *Quat. Int.* **2003**, *101–102*, 115–124. [CrossRef]
2. D'Alessandro, L.; Miccadei, E.; Piacentini, T. Morphotectonic study of the lower Sangro River valley (Abruzzi, Central Italy). *Geomorphology* **2008**, *102*, 145–158. [CrossRef]
3. Miccadei, E.; Piacentini, T.; Dal Pozzo, A.; La Corte, M.; Sciarra, M. Morphotectonic map of the Aventino-Lower Sangro valley (Abruzzo, Italy), scale 1:50,000. *J. Maps* **2013**, *9*, 390–409. [CrossRef]
4. Artoni, A. The Pliocene-Pleistocene stratigraphic and tectonic evolution of the Central sector of the Western Periadriatic Basin of Italy. *Mar. Pet. Geol.* **2013**, *42*, 82–106. [CrossRef]
5. Di Bucci, D.; Angeloni, P. Adria Seismicity and sismotectonics: Review and critical discussion. *Mar. Pet. Geol.* **2013**, *42*, 182–190. [CrossRef]
6. Kastelic, V.; Vannoli, P.; Burrato, P.; Fracassi, U.; Tiberti, M.M.; Valenzise, G. Seismogenic sources in the Adriatic Domain. *Mar. Pet. Geol.* **2013**, *42*, 191–213. [CrossRef]
7. Rovida, A.; Locati, M.; Camassi, R.; Lolli, B.; Gasperini, P. *CPTI15—2015 Version of the Parametric Catalogue of Italian Earthquakes*; INGV: Rome, Italy, 2016.
8. Gasparini, C.; Conte, S.; Vannucci, C. *Bollettino Macrosismico 2001–2005*; [CD-ROM]; INGV: Rome, Italy, 2011.
9. D'Agostino, N.; Jackson, J.A.; Dramis, F.; Funiciello, R. Interactions between mantle upwelling, drainage evolution and active normal faulting: An example from central Apennines (Italy). *Geophys. J. Int.* **2001**, *141*, 475–497. [CrossRef]
10. Pizzi, A. Plio-Quaternary uplift rates in the outer zone of the central Apennines fold-and-thrust belt, Italy. *Quat. Int.* **2003**, *101–102*, 229–237. [CrossRef]
11. Ascione, A.; Cinque, A.; Miccadei, E.; Villani, F.; Berti, C. The Plio-Quaternary uplift of the Apennine chain: New data from the analysis of topography and river valleys in Central Italy. *Geomorphology* **2008**, *101–102*, 105–108. [CrossRef]
12. Piacentini, T.; Miccadei, E. The role of drainage systems and intermontane basins in the Quaternary landscape of the Central Apennines chain (Italy). *Rend. Lincei-Sci. Fis. Nat.* **2014**, *25*, 139–150. [CrossRef]

13. Della Seta, M.; Del Monte, M.; Fredi, P.; Miccadei, E.; Nesci, O.; Pambianchi, G.; Piacentini, T.; Troiani, F. Morphotectonic evolution of the Adriatic piedmont of the Apennines: An advancement in the knowledge of the Marche-Abruzzo border area. *Geomorphology* **2008**, *102*, 119–129. [CrossRef]
14. Bracone, V.; Amorosi, A.; Aucelli, P.P.C.; Rosskopf, C.M.; Scarciglia, F.; Di Donato, V.; Esposito, P. The Pleistocene tectonosedimentary evolution of the Apenninic foreland basin between Trigno and Fortore rivers (Southern Italy) through a sequence stratigraphic perspective. *Basin Res.* **2012**, *24*, 213–233. [CrossRef]
15. Aucelli, P.P.C.; Faillace, P.I.; Rosskopf, C.M. Evoluzione geomorfologica del tratto finale del fondovalle del fiume Biferno (Molise) dal 1800 ad oggi. *Boll. Soc. Geog. Ital.* **2009**, *87*, 367–378.
16. Aucelli, P.P.C.; Cinque, A.; Rosskopf, C. Geomorphologic map of the Trigno basin (Italy): Explanatory notes. *Geogr. Fis. Din. Quat.* **2001**, *24*, 3–12.
17. Nesci, O.; Savelli, D. Diverging drainage in the Marche Apennines (central Italy). *Quat. Int.* **2003**, *101–102*, 203–209. [CrossRef]
18. Pazzaglia, F.J.; Brandon, M.T. A fluvial record of long-term steady-state uplift and erosion across the Cascadia forearc high, Western Washington State. *Am. J. Sci.* **2001**, *301*, 385–431. [CrossRef]
19. Giaconia, F.; Booth-Rea, G.; Martínez-Martínez, J.M.; Azañón, J.M.; Pérez-Peña, J.V. Geomorphic analysis of the Sierra Cabrera, an active pop-up in the constrictional domain of conjugate strike-slip faults: The Palomares and Polopos fault zones (eastern Betics, SE Spain). *Tectonophysics* **2012**, *580*, 27–42. [CrossRef]
20. Giaconia, F.; Booth-Rea, G.; Martínez-Martínez, J.M.; Azañón, J.M.; Pérez-Peña, J.V.; Pérez-Romero, J.; Villegas, I. Geomorphic evidence of active tectonics in the Sierra Alhamilla (eastern Betics, SE Spain). *Geomorphology* **2012**, *145*, 90–106. [CrossRef]
21. Ferrater, M.; Booth-Rea, G.; Pérez-Peña, J.V.; Azañón, J.M.; Giaconia, F.; Masana, E. From extension to transpression: Quaternary reorganization of an extensional-related drainage network by the Alhama de Murcia strike-slip fault (eastern Betics). *Tectonophysics* **2015**, *663*, 33–47. [CrossRef]
22. Molin, P.; Fubelli, G. Morphometric evidence of the topographic growth of central Apennines. *Geog. Fis. Din. Quat.* **2005**, *28*, 47–61.
23. Clermonté, J. Une contribution a l'étude géologique des formations molisanes du basin de Sangro (Italie centro-méridionale). *Boll. Soc. Geol.* **1969**, *7*, 830–840. [CrossRef]
24. Patacca, E.; Scandone, P. Geology of the Southern Apennines. *Boll. Soc. Geol. Ital.* **2007**, *7*, 75–119.
25. Ghisetti, F.; Vezzani, L.; Festa, A. *Note Illustrative Della Carta Geologica del Molise (Campobasso, Italy), Scala 1:100,000*; Litografia Geda: Nichelino, Italy, 2004.
26. Di Bucci, D. Rapporti tra piattaforme carbonatiche e «Alloctono» lungo la media valle del Sangro. *Mem. Soc. Geol. Ital.* **1995**, *11*, 443–463.
27. Di Bucci, D. *Carta Geologica dei Rilievi Circostanti la Media Valle del F. Sangro: La zona di M. Campo e la Struttura Pizzoferrato-Castel di Sangro*; Dipartimento di Scienze Geologiche: Rome, Italy, 1995.
28. Corrado, S.; Di Bucci, D.; Naso, G.; Butler, R.W.H. Thrusting and strike-slip tectonics in Alto Molise region (Italy): Implications for the Neogene-Quaternary evolution of the Central Apennine orogenic system. *J. Geol. Soc. Lond.* **1997**, *154*, 679–688. [CrossRef]
29. Corrado, S.; Di Bucci, D.; Naso, G.; Damiani, A.V. Rapporti tra le grandi unità stratigrafico-strutturali dell'Alto Molise (Appennino centrale). *Boll. Soc. Geol. Ital.* **1998**, *117*, 761–776.
30. Galadini, F.; Messina, P. Characterization of the recent tectonics of the Upper Sangro River Valley (Abruzzi Apennine, Central Italy). *Ann. Geofis.* **1993**, *36*, 277–285.
31. Di Bucci, D.; Tozzi, M. La "linea Ortona-Roccamonfina": Revisione dei dati esistenti e nuovi contributi per il settore settentrionale (media Valle del Sangro). *Studi Geol. Camerti* **1992**, *2*, 397–406.
32. Patacca, E.; Scandone, P.; Bellatalla, M.; Perilli, N.; Santini, U. La zona di giunzione tra l'arco appenninico settentrionale e l'arco appenninico meridionale nell'Abruzzo e nel Molise. *Studi Geol. Camerti* **1991**, *2*, 417–441.
33. Patacca, E.; Scandone, P.; Di Luzio, E.; Cavinato, G.P.; Parotto, M. Structural architecture of the central Apennines: Interpretation of the CROP 11 seismic profile from the Adriatic coast to the orographic divide. *Tectonics* **2008**, *27*. [CrossRef]
34. Capelli, G.; Miccadei, E.; Raffi, R. Fluvial dynamics in the Castel di Sangro plain: Morphological changes and human impact from 1875 to 1992. *Catena* **1997**, *30*, 295–309. [CrossRef]
35. Aucelli, P.P.C.; Cavinato, G.P.; Cinque, A. Geomorphological evidence of Pliocene-Quaternary tectonics in the Adriatic piedmont of the Abruzzi Apennines. *Il Quat.-Ital. J. Quat. Sci.* **1996**, *9*, 299–302.

36. Demangeot, J. *Geomorphologie des Abruzzes Adriatiques*; Edition du Centre National de la Recherche Scientifique (Paris): Paris, France, 1965; pp. 1–403.
37. Ascione, A.; Miccadei, E.; Villani, F.; Berti, C. Morphostructural setting of the Sangro and Volturno rivers divide area (Central-Southern Apennines, Italy). *Geogr. Fis. Dinam. Quat.* **2007**, *30*, 13–29.
38. Currado, C.; Fredi, P. Morphometric parameters of drainage basins and morphotectonic setting of western Abruzzo. *Mem. Soc. Geol. Ital.* **2000**, *55*, 411–419.
39. Ciccacci, S.; D'Alessandro, L.; Dramis, F.; Miccadei, E. Geomorphologic Evolution and Neotectonics of the Sulmona Intramontane Basin (Abruzzi, Apennine, Central Italy). *Z. Geomorphol.* **1999**, *118*, 27–40.
40. Miccadei, E.; Piacentini, T.; Esposito, G.; Berti, C.; Mancinelli, V. Morphotectonic map of the Tasso Stream-Sagittario River valley (Central Apennines, Italy). *J. Maps*. under review.
41. Mayer, L.; Menichetti, M.; Nesci, O.; Savelli, D. Morphotectonic approach to the drainage analysis in the North Marche region, central Italy. *Quat. Int.* **2003**, *101–102*, 157–167. [CrossRef]
42. Spagnolo, M.; Pazzaglia, F.J. Testing the geological influences on the evolution of river profiles: A case from northern Apennines (Italy). *Geogr. Fis. Dinam. Quat.* **2005**, *28*, 103–113.
43. Miccadei, E.; Piacentini, T.; Buccolini, M. Long-term geomorphological evolution in the Abruzzo area, Central Italy: Twenty years of research. *Geol. Carpathica* **2017**, *68*, 19–28. [CrossRef]
44. Patacca, E.; Scandone, P.; Sartori, R. Tyrrhenian basin and Apenninic arcs: Kinematic relations since Late Tortonian times. *Mem. Soc. Geol. Ital.* **1990**, *45*, 425–451.
45. Parotto, M.; Praturlon, A. The Southern Apennine arc. In *Geology of Italy*; Crescenti, U., D'Offizi, S., Merlino, S., Sacchi, L., Eds.; Italian Geological Society: Rome, Italy, 2004; pp. 33–58.
46. Vezzani, L.; Festa, A.; Ghisetti, F.C. Geology and tectonic evolution of the Central-Southern Apennines, Italy. *Geol. Soc. Am.* **2010**, *469*, 1–58.
47. Ascione, A.; Cinque, A. Tectonics and erosion in the long term relief history of the Southern Apennines (Italy). *Z. Geomorphol. Suppl.* **1999**, *118*, 1–16.
48. Nesci, O.; Savelli, D.; Troiani, F. Types and development of stream terraces in the Marche Apennines (Central Italy): A review and remarks on recent appraisals. *Geomorphol. Relief Process. Environ.* **2012**, *2*, 215–238. [CrossRef]
49. Calista, M.; Miccadei, E.; Pasculli, A.; Piacentini, T.; Sciarra, M.; Sciarra, N. Geomorphological features of the Montebello sul Sangro large landslide (Abruzzo, Central Italy). *J. Maps* **2016**, *12*, 882–891. [CrossRef]
50. Miccadei, E.; Mascioli, F.; Ricci, F.; Piacentini, T. Geomorphology of soft clastic rock coasts in the Mid Western Adriatic Sea (Abruzzo, Italy). *Geomorphology*. accepted.
51. Devoti, R.; D'Agostino, N.; Serpelloni, E.; Pietrantonio, G.; Riguzzi, F.; Avallone, A.; Cavaliere, A.; Cheloni, D.; Cecere, G.; D'Ambrosio, C.; et al. A combined velocity field of the mediterranean region. *Ann. Geophys.* **2017**, *60*, 0215. [CrossRef]
52. Chiaraluce, L.; Di Stefano, R.; Tinti, E.; Scognamiglio, L.; Michele, M.; Casarotti, E.; Cattaneo, M.; De Gori, P.; Chiarabba, C.; Monachesi, G.; et al. The 2016 central Italy seismic sequence: A first look at the mainshocks, aftershocks, and source models. *Seismol. Res. Lett.* **2017**, *88*, 757–771. [CrossRef]
53. ISIDe Working Group, Version 1.0. Available online: http://cnt.rm.ingv.it/iside (accessed on 7 September 2018). [CrossRef]
54. C Cruppo di Lavoro. *Gruppo di Lavoro CPTI Catalogo Parametrico dei Terremoti Italiani. 2004 (CPTI04)*; INGV: Bologna, Italy, 2004.
55. Locati, M.; Camassi, R.; Rovida, A.; Ercolani, E.; Bernardini, F.; Castelli, V.; Caracciolo, C.H.; Tertulliani, A.; Rossi, A.; Azzaro, R.; et al. *DBMI15, The 2015 Version of the Italian Macroseismic Database*; INGV: Rome, Italy, 2016.
56. Elter, P.; Grasso, M.; Parotto, M.; Vezzani, L. Structural setting of the Apennine-Maghrebian thrust belt. *Episodes* **2003**, *26*, 205–211.
57. Dramis, F. The role of long-range tectonic uplift in the genesis of the Apennine relief. *Studi Geol. Camerti* **1993**, *1*, 9–15.
58. Nesci, O.; Savelli, D. Successioni alluvionali terrazzate nell'Appennino nordmarchigiano. *Geog. Fis. Din. Quat.* **1991**, *14*, 149–162.
59. Nesci, O.; Savelli, D.; Veneri, F. Terrazzi vallivi e superfici di spianamento nell'evoluzione del rilievo appenninico nord-marchigiano. *Studi Geol. Camerti* **1992**, *1*, 175–180.
60. Di Celma, C.; Farabollini, P.; Moscatelli, U. Landscape, settlement and roman cadastres in the lower Sangro valley (Italy). *Geoarchaeol. Landsc. Class. Antiq.* **2000**, *5*, 23–34.

61. SGI. *Geological Map of Italy, Scale 1:100,000, Sheet 161 "Isernia"*; ISPRA: Rome, Italy, 1971.
62. SGI. *Geological Map of Italy, Scale 1:100,000, Sheet 153 "Agnone"*; ISPRA: Rome, Italy, 1971.
63. ISPRA. *Geological Map of Italy, Scale 1:50,000, Sheet 372 "Vasto"*; ISPRA: Rome, Italy, 2010.
64. ISPRA. *Geological Map of Italy, Scale 1:50,000, Sheet 393 "Trivento"*; ISPRA: Rome, Italy, 2011.
65. Allocca, V.; Celico, F.; De Vita, P.; Fabbrocino, S. Idrodinamica sotterranea in successioni carbonatiche in facies di bacino: L'area campione di Monte Campo (Molise, Italia meridionale). *Ital. J. Eng. Geol. Environ.* **2006**, *2*, 5–22.
66. Strahler, A.N. Quantitative analysis of watershed geomorphology. *Am. Geophys. Union Trans.* **1957**, *38*, 913–920. [CrossRef]
67. Avena, G.C.; Giuliano, G.; Lupia Palmieri, E. Sulla valutazione quantitativa della gerarchizzazione ed evoluzione dei reticoli fluviali. *Boll. Soc. Geol. Ital.* **1967**, *86*, 781–196.
68. Strahler, A.N. Dynamic basis of geomorphology. *Geol. Soc. Am. Bull.* **1952**, *63*, 923–938. [CrossRef]
69. Ciccacci, S.; D'Alessandro, L.; Fredi, P.; Lupia Palmieri, E. Relation between morphometric characteristics and denudational processes in some drainage basins of Italy. *Z. Geomorphol.* **1992**, *36*, 53–67.
70. Wobus, C.; Whipple, K.; Kirby, E.; Snyder, N.; Johnson, J.; Spyropolou, K.; Sheehan, D. Tectonics from topography: Procedures, promise and pitfalls. *Geol. Soc. Am.* **2006**, *398*, 5–74.
71. Burbank, D.W.; Anderson, R.S. *Tectonic Geomorphology*, 2nd ed.; Wiley-Blackwell: Hokken, NJ, USA, 2011.
72. Ahnert, F. Local relief and height limits of mountain ranges. *Am. J. Sci.* **1984**, *284*, 1035–1055. [CrossRef]
73. Ciccacci, S.; D'Alessandro, L.; Fredi, P.; Lupia Palmieri, E. Contributo dell'analisi geomorfica quantitativa allo studio dei processi di denudazione nel bacino idrografico del Torrente Paglia (Toscana meridionale—Lazio settentrionale). *Suppl. Geogr. Fis. Dinam. Quat.* **1988**, *1*, 171–188.
74. Keller, E.A.; Printer, N. *Active Tectonics: Earthquakes, Uplift, and Landscape*, 2nd ed.; Prentice Hall: Old Tappan, NJ, USA, 2001.
75. Pérez-Peña, J.V.; Azañón, J.M.; Azor, A. CalHypso: An ArcGIS extension to calculate hypsometric curves and their statistical moments. Applications to drainage basin analysis in SE Spain. *Comput. Geosci.* **2009**, *35*, 1214–1223. [CrossRef]
76. Ciccacci, S.; Fredi, P.; Lupia Palmieri, E.; Pugliese, F. Contributo dell'analisi geomorfica quantitativa alla valutazione dell'entità dell'erosione nei bacini fluviali. *Boll. Soc. Geol. Ital.* **1980**, *99*, 455–516.
77. Grauso, S. Carta dell'indice di erosione dell'alto bacino del Fiume Agri. *Doc. Del Territ.* **1994**, *28–29*, 46–53.
78. Agnesi, V.; Cappadonia, C.; Conoscenti, C.; Di Maggio, C.; Marker, M.; Rotigliano, E. Valutazione dell'erosione del suolo nel bacino del Fiume San Leonardo (Sicilia Centro-Occidentale, Italia). In Proceedings of the Atti del Convegno Conclusivo del Progetto "Erosione idrica in Ambiente Mediterraneo: Valutazione Diretta e Indiretta in aree Sperimentali e Bacini idrografici", Florence, Italy, 17 December 2004; pp. 13–27.
79. Ciccacci, S.; Fredi, P.; Lupia Palmieri, E.; Salvini, F. An approach to the quantitative analysis of the relations between drainage pattern and fracture trend. *Int. Geomorphol.* **1986**, 49–68.
80. Belisario, F.; Del Monte, M.; Fredi, P.; Funiciello, R.; Lupia Palmieri, E.; Salvini, F. Azimuthal analysis of stream orientations to define regional tectonic lines. *Z. Geomorphol.* **1999**, *118*, 41–63.
81. Lupia Palmieri, E.; Ciccacci, S.; Civitelli, G.; Corda, L.; D'Alessandro, L.; Del Monte, M.; Fredi, P.; Pugliese, F. Geomorfologia quantitativa e morfodinamica del territorio abruzzese—I-IL bacino idrografico del Fiume Sinello. *Geogr. Fis. Din. Quat.* **1995**, *18*, 31–46.
82. Lupia Palmieri, E.; Centamore, E.; Ciccacci, S.; D'Alessandro, L.; Del Monte, M.; Fredi, P.; Pugliese, F. Geomorfologia quantitativa e morfodinamica del territorio abruzzese—II-IL bacino idrografico del Fiume Tordino. *Geogr. Fis. Din. Quat.* **1998**, *21*, 113–129.
83. Lupia Palmieri, E.; Biasini, A.; Caputo, C.; Centamore, E.; Ciccacci, S.; Del Monte, M.; Fredi, P.; Pugliese, F. Geomorfologia quantitativa e morfodinamica del territorio abruzzese—III-IL Bacino del Fiume Saline. *Geogr. Fis. Din. Quat.* **2001**, *24*, 157–176.
84. Centamore, E.; Ciccacci, S.; Del Monte, M.; Fredi, P.; Lupia Palmieri, E. Morphological and morphometric approach to the study of the structural arrangement of the North-Eastern Abruzzo (Central Italy). *Geomorphology* **1996**, *16*, 127–137. [CrossRef]
85. Kusak, M.; Kropacek, J.; Vilimek, V.; Scillaci, C. Analysis of the influence of tectonics on the evolution of valley networks based on SRTM DEM, Jemma River basin, Ethiopia. *Geogr. Fis. Dinam. Quat.* **2016**, *39*, 37–50.

86. Pellegrini, A.; Cura di, G.B.; Carton, A.; Castaldini, D.; Cavallin, A.; D'Alessandro, L.; Dramis, F.; Gentili, B.; Laureti, L.; Prestininzi, A.; Rodolfi, G. Proposta di legenda geomorfologica ad indirizzo applicativo. *Geogr. Fis. Din. Quat.* **1993**, *16*, 129–152.
87. SGN. Guida al rilevamento della Carta geomorfologica d'Italia, 1:50,000. In *Quaderni Serie III del Servizio Geologico Nazionale*; Servizio Geologico d'Italia: Rome, Italy, 1994; p. 4.
88. ISPRA. Guida alla rappresentazione cartografica della Carta geomorfologica d'Italia, 1:50,000. In *Quaderni Serie III del Servizio Geologico Nazionale*; Servizio Geologico d'Italia: Rome, Italy, 2007; p. 48.
89. ISPRA. Aggiornamento ed integrazione delle linee guida della Carta geomorfologica d'Italia in scala 1:50,000. In *Quaderni Serie III del Servizio Geologico Nazionale*; Servizio Geologico d'Italia: Rome, Italy, 2018; p. 98.
90. Miccadei, E.; Orrù, P.; Piacentini, T.; Mascioli, F.; Puliga, G. Geomorphological map of Tremiti Islands Archipelago (Puglia, Southern Adriatic Sea, Italy), scale 1:15,000. *J. Maps* **2012**, *8*, 74–87. [CrossRef]
91. Piacentini, T.; Urbano, T.; Sciarra, M.; Schipani, I.; Miccadei, E. Geomorphology of the floodplain at the confluence of the Aventino and Sangro rivers (Abruzzo, Central Italy). *J. Maps* **2015**, *12*, 443–461. [CrossRef]
92. Ambrosetti, P.; Bonadonna, F.P.; Bosi, C.; Carraro, F.; Cita, B.M.; Giglia, G.; Manetti, P.; Martinis, B.; Merlo, C.; Panizza, M.; et al. Proposta di un progetto operativo per l'elaborazione della carta neotettonica d'Italia. In *Progetto Finalizzato Geodinamica*; Rome, Italy, 1976; pp. 1–49.
93. Miccadei, E.; Paron, P.; Piacentini, T. The SW escarpment of the Montagna del Morrone (Abruzzi, Central Italy): Geomorphology of a fault-generated mountain front. *Geogr. Fis. Dinam. Quat.* **2004**, *27*, 55–87.
94. Miccadei, E.; Mascioli, F.; Piacentini, T. Quaternary geomorphological evolution of the Tremiti Islands (Puglia, Italy). *Quat. Int.* **2011**, *232*, 3–15. [CrossRef]
95. Miccadei, E.; Piacentini, T.; Gerbasi, F.; Daverio, F. Morphotectonic map of the Osento River basin (Abruzzo, Italy), scale 1:30,000. *J. Maps* **2012**, *8*, 62–73. [CrossRef]
96. ENEL. *Elementi di Neotettonica del Territorio Italiano*; ENEL–Aquater (Gruppo ENI): Rome, Italy, 1981; p. 94.
97. Goldsworthy, M.; Jackson, J. Active normal fault evolution in Greece revealed by geomorphology and drainage patterns. *J. Geol. Soc. Lond.* **2000**, *157*, 967–981. [CrossRef]
98. Gioia, D.; Schiattarella, M.; Mattei, M.; Nico, G. Quantitative morphotectonics of the Pliocene to Quaternary Auletta basin, southern Italy. *Geomorphology* **2011**, *134*, 326–343. [CrossRef]
99. D'Alessandro, L.; Del Sordo, L.; Buccolini, M.; Miccadei, E.; Piacentini, T.; Urbani, A. Analisi del dissesto da frana in Abruzzo. In *Il Progetto IFFI-Inventario dei Fenomeni Franosi in Italia: Metodologia e Risultati*; Rapporto APAT: Rome, Italy, 2007; pp. 463–692.